The role of rotation in the evolution of dynamo-generated magnetic fields in Super Earths

Jorge I. Zuluaga, Pablo A. Cuartas

Instituto de Física - FCEN, Universidad de Antioquia, Calle 67 No. 53-108, Medellín, Colombia

Abstract

Planetary magnetic fields could impact the evolution of planetary atmospheres and have a role in the determination of the required conditions for the emergence and evolution of life (planetary habitability). We study here the role of rotation in the evolution of dynamo-generated magnetic fields in massive Earth-like planets, Super Earths (1-10 $M_\oplus$). Using the most recent thermal evolution models of Super Earths (Gaidos *et al.*, 2010; Tachinami *et al.*, 2011) and updated scaling laws for convection-driven dynamos, we predict the evolution of the local Rossby number. This quantity is one of the proxies for core magnetic field regime, i.e. non-reversing dipolar, reversing dipolar and multipolar. We study the dependence of the local Rossby number and hence the core magnetic field regime on planetary mass and rotation rate. Previous works have focused only on the evolution of core magnetic fields assuming rapidly rotating planets, i.e. planets in the dipolar regime. In this work we go further, including the effects of rotation in the evolution of planetary magnetic field regime and obtaining global constraints to the existence of intense protective magnetic fields in rapidly and slowly rotating Super Earths. We find that the emergence and continued existence of a protective planetary magnetic field is not only a function of planetary mass but also depend on rotation rate. Low-mass Super Earths ($M \lesssim 2\,M_\oplus$) develop intense surface magnetic fields but their lifetimes will be limited to 2-4 Gyrs for rotational periods larger than 1-4 days. On the other hand and also in the case of slowly rotating planets, more massive Super Earths ($M \gtrsim 2\,M_\oplus$) have weak magnetic fields but their dipoles will last longer. Finally we analyze tidally locked Super Earths inside and outside the habitable zone of GKM stars. Using the results obtained here we develop a classification of Super Earths based on the rotation rate and according to the evolving properties of dynamo-generated planetary magnetic fields.

Keywords: Interiors, Magnetic fields, Thermal histories.

1. Introduction

The number of known exoplanets in the mass range between 1 and 10 $M_\oplus$ is growing (hereafter these objects will be called "Super Earths" or SEs following the classification by Valencia *et al.* (2006, 2007a)). At the time of writing, there are almost 46 confirmed planets in this mass range[1](Rivera *et al.*, 2005; Beaulieu *et al.*, 2006; Udry *et al.*, 2007; Mayor and Udry, 2008; Ribas *et al.*, 2008; Queloz *et al.*, 2009; Bonfils *et al.*, 2011; Lissauer *et al.*, 2011) and more than a few hundred SEs candidates are awaiting further analysis and confirmation (Borucki *et al.*, 2011). These discoveries have increased the interest to model and understand the geophysical properties of this type of planets (Valencia *et al.*, 2006, 2007a,b; Valencia and O'Connell, 2009; Seager *et al.*, 2007; Kaltenegger, 2010; Korenaga, 2010). The habitability of SEs, in particular those similar in composition and structure to the Earth, is an interesting topic in the field and several theoretical works

Email addresses: jzuluaga@fisica.udea.edu.co (Jorge I. Zuluaga), p.cuartas@fisica.udea.edu.co (Pablo A. Cuartas)

[1]For updates, please refer to http://exoplanet.eu

have paid special attention to this particular aspect of SEs properties (Grießmeier *et al.*, 2005, 2009, 2010; Selsis *et al.*, 2007; van Thienen *et al.*, 2007; von Bloh *et al.*, 2007; Lammer *et al.*, 2010).
Models of the interior structure of SEs have been extensively developed over the last 5 years (Valencia *et al.*, 2006, 2007a,b; Fortney *et al.*, 2007; Seager *et al.*, 2007; Selsis *et al.*, 2007; Sotin *et al.*, 2007; Adams *et al.*, 2008; Baraffe *et al.*, 2008; Grasset *et al.*, 2009). Although there are still open issues to be addressed, these models are giving us an understanding of global properties such as the mass-radius relationship and its dependence with planetary composition, as well as different geophysical phenomena such as mantle convection, degassing and plate tectonics (Olson, 2007; Papuc and Davies, 2008; Valencia *et al.*, 2007; Valencia and O'Connell, 2009; Korenaga, 2010). Recently several authors have studied in detail the thermal evolution and magnetic field properties of this type of planets (Gaidos *et al.*, 2010; Tachinami *et al.*, 2011; Driscoll and Olson, 2011).
Planetary magnetic fields would likely play a role in planetary habitability (von Bloh *et al.*, 2007; Grießmeier *et al.*, 2005, 2009, 2010; van Thienen *et al.*, 2007; Lammer *et al.*, 2010). Understanding the conditions for the emergence and long term evolution of a protective planetary magnetic field (hereafter PMF) is crucial to evaluate the complex conditions for habitability of SEs. The same conditions could also be applied to evaluate the habitability of exomoons around extrasolar giant planets (Kaltenegger *et al.*, 2010).
The current understanding of PMF emergence and evolution in SEs arises from thermal evolution models for the Earth (Stevenson, 2003; Labrosse, 2003, 2007a,b; Nimmo, 2009; Aubert *et al.*, 2009; Breuer *et al.*, 2010) and scaling laws for convection-driven dynamos obtained from extensive numerical simulations (Christensen and Aubert, 2006; Olson and Christensen, 2006; Aubert *et al.*, 2009; Christensen *et al.*, 2009; Christensen, 2010). Two recent works studied the problem of PMF evolution in SEs by developing detailed models of planetary thermal evolution (Gaidos *et al.*, 2010; Tachinami *et al.*, 2011). Both works have paid special attention to different but complementary aspects of the problem. Gaidos *et al.* (2010) uses a model of the structure of the planetary core and its thermal evolution (hereafter the *Core Thermal Evolution* or *CTE model*). On the other hand Tachinami *et al.* (2011) uses the Mixing Length Theory adapted to planetary conditions to model mantle convection with a detailed treatment of its rheological properties (hereafter the *Mantle based Thermal Evolution model* or *MTE model*). Although thermal evolution models for the Earth, other terrestrial planets and even SEs have been developed in the past (Stevenson, 2003; Labrosse, 2003, 2007a; Papuc and Davies, 2008; Nimmo, 2009; Breuer *et al.*, 2010), the CTE and MTE models give the first detailed description aimed at studying dynamo-generated magnetic fields of extrasolar terrestrial planets.
We use the results of the CTE and MTE models to study the role of rotation in the evolution of PMF in SEs. We focus on the evolution of the regime of the core magnetic field (CMF) which can be broadly classified as non-reversing dipolar, reversing dipolar and multipolar. For this purpose we compute the *local Rossby number*, one of the proxies for CMF regime, as a function of the rotation period and planetary mass. Using this property we predict the long term evolution of the surface PMF in rapidly and slowly rotating planets.
In section 2 we summarize the most important results of the CTE and MTE models. Section 3 presents the scaling laws for convection-driven dynamos used to predict the properties of the CMF. In section 4 we present a general procedure to compute the CMF intensity in the dipolar and multipolar regimes including an implicit dependence on rotation rate. In section 5 we present the results of applying the procedure devised here to predict the maximum dipolar component of the field in SEs with different periods of rotation and thermal histories as predicted by the CTE and MTE models. Section 6 is devoted to discuss the limitations of our procedure and the implications of our results. A summary, concluding remarks and future prospects are presented in section 7. For reference a list of the symbols and the physical quantities used in this work are presented in Table 1.

2. Thermal evolution models of SEs

2.1. Planetary thermal evolution

The evolution and long-term survival of a dynamo-generated PMF[2] strongly depends on the thermal history of the planet. The energy sources and the amount of energy available for dynamo action change in time as the planet cools and, in some cases, its core solidifies.

Before we present the predicted properties of planetary dynamos and the role of rotation in the evolution of those properties, we present the most recent advances in the study of thermal evolution of SEs. Thermal evolution models are the starting point of any dynamo evolutionary model. The onset of dynamo action in the core requires values of the magnetic Reynolds number beyond a given threshold $Re_m > 40$ (Olson and Christensen, 2006). The strength of the dynamo and hence the intensity of the generated magnetic field are essentially set by the available convective power Q_{conv} (Olson and Christensen, 2006). An important role is also played by the size of the convective region that in core dynamos is given by the difference between the radius of the outer core and the radius of the solid inner core. In the thermal evolution models studied here (Gaidos *et al.*, 2010; Tachinami *et al.*, 2011) Q_{conv} is estimated in two different ways. In the CTE model this quantity is obtained by solving first the thermal equilibrium equations for the core and mantle and then computing the ohmic dissipation from the balance between entropy sources (radioactive decay, secular cooling, sensible heat, latent heat and other sources of buoyancy) and sinks (heat conduction, ohmic dissipation and other sources of dissipation) (Lister, 2003; Labrosse, 2003, 2007a; Nimmo, 2009; Gaidos *et al.*, 2010). In the MTE model, Q_{conv} is estimated solving first the thermal transport equations in the mantle and the core and computing the difference between the heat that comes out of the core-mantle boundary (CMB) and the amount of energy transported by conduction through it (Tachinami *et al.*, 2011). Important differences between the CTE and MTE models arise from the way Q_{conv} is estimated (see section 2.3). In the following sections we discuss in detail some of the specific features of the CTE and MTE models.

2.2. The CTE model

Gaidos *et al.* (2010) (CTE model) solved the entropy equilibrium equations in the core assuming adequate initial and boundary conditions and a parametrized description of the density and temperature profiles. They used a basic model of the heat transport inside the mantle to compute the total planetary energy balance and calculate the relevant quantities required to describe the thermal evolution of planets between 1 and 4.8 $M_\oplus$. Assuming rapidly rotating planets, they also predicted the evolution of the PMF intensity from the dynamo scaling laws originally developed by Christensen and Aubert (2006) and later improved by Aubert *et al.* (2009) and Christensen (2010). In Table 2 we summarize some of the results presented in Fig. 8 of Gaidos *et al.* (2010).

In the CTE model the interaction between the core thermal structure, the existence and growth of a solid inner core, the mantle properties, the onset of plate tectonics and the surface temperature, determine the existence and survival of an intense PMF in SEs. A robust upper bound, close to 2 $M_\oplus$ (low-mass SEs) to have strong protective PMF is obtained with this model. Planets with masses larger than this limit will not cool enough to develop a solid inner core, a condition that considerably boosts the magnetic field intensity in lighter and cooler planets. As a consequence, massive SEs ($M \gtrsim 2\,M_\oplus$) develop a decaying weak magnetic field. In this case the dynamo is shut down early when the convective power falls below the condition for dynamo action. These results depend strongly on the existence or not of mobile lids (plate tectonics, PT).

2.3. The MTE model

Tachinami *et al.* (2011) (MTE model) pays special attention to the role that the mantle have in the extraction of heat from the core, taking into account its particular rheological properties. They use the Mixing Length Theory modified for solid planets in order to compute the energy transported by convection in the mantle and the energy budget at the CMB for planets with masses between 0.1 and 10 $M_\oplus$. They assume a

[2]It is important to stress that we are considering in this work magnetic fields generated by dynamo action in a liquid metallic core. Other fluid shells (liquid, ice or gaseous mantles) may sustain other type of dynamos out of the scope of this work.

planet with a mantle-core mass ratio similar to the Earth's. The MTE model includes parameters like the rheological properties of the mantle (especially important is the activation volume V^* that determines the viscosity dependence on pressure and temperature) and the temperature contrast ΔT_{CMB} in the boundary layer between the convecting mantle and the CMB. After solving the mantle and core coupled thermal transport equations, they compute, for different model configurations, the heat flux at the CMB F_{CMB}, the heat conducted along the adiabat F_{cond} at the CMB, and the solid inner core radius R_{ic} as a function of time. To predict the PMF intensity and its lifetime they estimate the convective power as $Q_{conv} = (F_{CMB} - F_{cond}) \times 4\pi R_c^2$ where R_c is the radius of the outer core. As in the case of the CTE model they assume rapidly rotating planets, i.e. planets with a dynamo operating in the dipolar regime.
Two important new predictions arise from the MTE model: (1) thermal evolution is affected by the strong dependence on pressure and temperature of mantle viscosity and (2) the intensity and lifetime of the PMF would strongly depend on the initial temperature profile which is characterized by the parameter ΔT_{CMB}, the temperature contrast between the core and the lower mantle; it is a property mainly determined by the early accretion and differentiation history of the planet. Larger values of the initial temperature contrast ΔT_{CMB}, created for example by a violent accretion history, would favor the appearance of an intense and long-lived PMF. They found that by doubling ΔT_{CMB} from 1000 K to 2000 K the dynamo lifetime in massive SEs ($M > 2\,M_\oplus$) is almost one order of magnitude larger. It should be stressed that the CTE model also studied the effects of different thermal profiles by considering the cases of non-habitable surface temperatures. This would be the case of highly irradiated planets (not considered in the MTE model). In this case the conclusions drawn by both models about the effect of different temperature profiles on the PMF properties, were essentially the same.

2.4. Comparison of the models

The results of the CTE and MTE models point broadly in the same direction: SEs with masses less than approximately 2 $M_\oplus$ seem to have properties better suited for the development of strong and long-lived PMFs. The ~ 2 $M_\oplus$ threshold is the most robust prediction of these models. In the CTE model the reason that limits the capability of low-mass SEs to sustain a dynamo is the early cooling and stratification of the core. On the other hand, the MTE model predicts a strong effect of the pressure-dependent viscosity in the thermal evolution of the planet, which limits the capacity of mantle convection to extract heat efficiently from the core, especially in the case of massive planets.

We want to highlight that the evolution of the PMF properties predicted by the CTE and MTE models were obtained for planets with short, but not specified, periods of rotation, i.e. planets with dynamos operating in the dipolar regime. For rapidly rotating dynamos, the reference dynamo models used by the CTE and MTE models (Christensen and Aubert, 2006; Olson and Christensen, 2006; Aubert *et al.*, 2009; Christensen *et al.*, 2009) predict that the magnetic energy density and hence the magnetic field intensity, depends weakly on the rotation rate. The still open question regarding the effect that long periods of rotation would have in the PMF properties predicted by these models. Particularly interesting is to study the effect that rotation would have in the determination of dynamo regime. It would be equally interesting to estimate the value for the rotation rate where the rapid rotation approximation could be used. These questions are particularly relevant in the case of tidally locked SEs as will be discussed in section 5.3.
For the purpose of this work a limited subset of model configurations included in the CTE and MTE models and highlighted in Table 2 have been selected. The final goal is to study the effect of rotation in the evolution of long-lived protective PMF in habitable SEs[3]. The chosen configurations must meet two criteria: (1) habitable surface temperatures (288 K in the CTE model, 300 K in the MTE model) and (2) long-lived and intense PMF. In the CTE case the latter condition requires the existence of plate tectonics. Since we are interested in computing upper bounds to surface PMF intensities, given the same set of planetary properties (mass, composition, surface temperature, etc.) the case where plate tectonics arises will be the best suited to set these bounds.

[3]A solid planet is considered habitable if the teperature on its surface is enough to maintain liquid water on the planet surface (see Kasting *et al.* (1993) and references there in).

For planets with 1 $M_\oplus$ the configuration selected in the CTE and MTE models must reproduce the intensity of the present Earth's PMF and be consistent with the thermal evolution of the Earth, i.e. they must predict correctly the time of inner core nucleation.
In order to understand the role of rotation in the PMF evolution in SEs we have to take into account the dynamo properties that depend on rotation rate. To achieve this we shortly review the relationship between the thermal state of the planet and the properties of the dynamo in the following section.

3. Properties of convection-driven dynamos

3.1. Scaling laws

It has been suggested from numerical dynamo experiments that the global properties of convection-driven dynamos can be expressed in terms of simple power-law functions of a modified Rayleigh number (Christensen and Aubert, 2006; Olson and Christensen, 2006; Aubert *et al.*, 2009; Christensen *et al.*, 2009). The scaling relationships found by these works involves the convective power Q_{conv}, the core geometry, i.e. the outer core radius and the vertical height of the liquid core $D = R_c - R_{ic}$ (R_{ic} is the inner core radius), the rotation rate Ω and other properties of the core.
The power-based scaling laws used in this work are expressed using the recent parametrization by Aubert *et al.* (2009) where the properties of the dynamo are scaled in terms of the adimensional convective power density p,

$$p = \frac{Q_{conv}}{\Omega^3 D^2 \overline{\rho}_c V} \tag{1}$$

Here $\overline{\rho}_c$ and V are the average density and total volume of the convecting region respectively. The use of p in the scaling laws, instead of the mass anomaly related Rayleigh number Ra_Q, is justified from physical and numerical grounds (see section 2.2 in Aubert *et al.* (2009)).
Two basic adimensional quantities have been used to characterize the global properties of a dynamo (Christensen and Aubert, 2006; Christensen, 2010): the *Lorentz number Lo* and the *local Rossby number* Ro_l. *Lo* is the adimensional magnetic field strength and is defined by Eq. (22) in Aubert *et al.* (2009) as

$$Lo = \frac{B_{rms}}{\sqrt{\overline{\rho}_c \mu_o} \Omega D} \tag{2}$$

where $B_{rms} = (1/V) \int B^2 dV$, is the rms amplitude of the magnetic field inside the convecting shell with volume V, μ_o is the magnetic permeability. Ro_l measures the ratio of inertial to Coriolis forces and is defined as

$$Ro_l = \frac{U_{rms}}{\Omega L} \tag{3}$$

where U_{rms} and $L \sim D/\overline{l}$ are the characteristic convective velocity and length scale respectively ($\overline{l}$ is the mean spherical harmonic degree of the kinetic energy spectrum). By definition Ro_l will be large for vigorous convection, small characteristic length scale or slowly rotating dynamos. Conversely rapid rotating dynamos, large characteristic length scale or a weak convection will produce small values of Ro_l.
Numerical dynamo experiments covering a wide range of physical properties and boundary conditions (Christensen and Aubert, 2006; Olson and Christensen, 2006; Aubert *et al.*, 2009; Christensen *et al.*, 2009; Christensen, 2010) have found the following scaling relationships for *Lo* and Ro_l (Eqs. (22) and (30) in Aubert *et al.* 2009):

$$Lo = c_{Lo} f_{ohm}^{1/2} p^{1/3} \tag{4}$$

$$Ro_l^* \equiv \frac{Ro_l}{(1+\chi)} = c_{Rol}\, p^{1/2} E^{-1/3} (Pr/Pm)^{1/5} \tag{5}$$

where f_{ohm} is the fraction of the available convective power converted to magnetic field and lost by ohmic dissipation, $\chi \equiv R_{ic}/R_c$, $E = \nu/(\Omega D^2)$ is the (viscous) Ekman number (ν is the viscous diffusivity) and $Pr/Pm = \lambda/\kappa$ is the ratio of the Prandtl to magnetic Prandtl number (λ and κ are the magnetic and thermal diffusivities respectively). For simplicity we have approximated the scaling law exponents to the ratio of the smallest integers as suggested by Olson and Christensen (2006). We have also introduced here the *modified local Rossby number* Ro_l^* following the suggestion by Aubert *et al.* (2009).
The values of the constants c_{Lo} and c_{Rol} are obtained by fitting the results of numerical dynamo experiments with different boundary conditions. It should be noted that although the scaling law for Lo in Eq. (4) has been generally tested only for dipolar dynamos, recently Christensen (2010) has found that the magnetic energy $E_m \sim Lo^2$ still follows a 2/3-scaling law for multipolar dynamos. In that case the constant c_{Lo} fitting the properties of multipolar dynamos is smaller than in the dipolar case by a factor ≈ 0.6 (Christensen, 2010).
Particulary interesting is that the scaling law for Lo provides a simple way to scale B_{rms} with p irrespective of the dynamo regime. Using the definition in Eq. (2) and the scaling law in Eq. (4) we can write down an expression for the magnetic field intensity (see Eq. 22 in Aubert *et al.* (2009))

$$B_{rms} = c_B f_{ohm}^{1/2} (\overline{\rho}_c \mu_o)^{1/2} \Omega D p^{1/3} \tag{6}$$

Given the fact that by definition $p \propto \Omega^{-1/3}$ (see Eq. (1)), we find that B_{rms} is almost independent[4] of rotation rate both in the dipolar and multipolar regimes. However, the dipolar component of the field will depend on rotation rate through the local Rossby number in the case of reversing dipolar and multipolar dynamos (see section 4).

3.2. Dynamo regimes

Dynamos could be broadly classified according to the power spectrum of the magnetic field at CMB in two groups: dipolar dominated dynamos, i.e. dynamos where the dipolar component dominate over other higher order components, and multipolar dynamos that have a flatter spectrum or a weak dipolar contribution.
Quantitatively the dipolarity of core dynamos is commonly measured using the ratio f_{dip} of the mean dipole field strength at the CMB, $\overline{B}_{dip}$, to the rms field strength summed up to the harmonic degree 12 at the same surface $\overline{B}_{CMB}$,

$$f_{dip} = \frac{\overline{B}_{dip}}{\overline{B}_{CMB}}. \tag{7}$$

It has been assumed that dipolar dominated dynamo have $f_{dip} > 0.35$ (Aubert *et al.*, 2009; Christensen, 2010). Conversely when $f_{dip} \lesssim 0.35$ the dynamo is classified as multipolar. Another useful quantity to measure the degree of dipolarity is the relation b_{dip} between the rms strength of the field in the shell volume B_{rms} and the dipolar component at the CMB,

$$b_{dip} = \frac{B_{rms}}{\overline{B}_{dip}}. \tag{8}$$

Large values of b_{dip} are typically a signature of a multipolar dynamo although in numerical experiments dipolar dominated dynamos could also have large b_{dip} values. However, the contrary is not true: low values of b_{dip} are only found in dipolar dominated dynamos. Typical values of b_{dip} can be found in the lower panel of Fig. (1).
For the present conditions of the geodynamo $f_{dip\oplus} \simeq 0.63$ ($B_{dip\oplus} = 0.263$ mT and $B_{CMB\oplus} = 0.42$ mT (Olson, 2007)) placing it in the dipolar regime. However, the value of b_{dip} for the geodynamo is largely uncertain. Estimates of B_{rms} (required to compute b_{dip}) can be computed applying proper scaling laws. Using for example the Elsasser number criterion an estimate of $B_{rms\oplus} \sim 4$ mT is obtained (Roberts and Glatzmaier,

[4]It should be recalled that the exact value of the exponent of p in the scaling law for Lo is close to 1/3 but not exactly equal to this value.

2000; Olson, 2007). Dividing by $B_{dip\oplus} = 0.263$ we obtain $b_{dip\oplus} \sim 15$. On the other hand power based scaling laws as those used in this work (Christensen, 2010) could be used to predict $B_{rms} \sim 1.5$ mT (see e.g. Aubert *et al.* 2009) and therefore $b_{dip\oplus} \sim 5$. Both values are also compatible with those found in numerical dipolar dominated dynamos (see lower panel of Fig. 1).
Finally dynamos could be stable in the long-term or exhibit a reversing behavior (see Amit *et al.* (2010) and references there in). In most cases dipolar dynamos do not reverse and reversing dynamos are multipolar, with very little (if any) overlap between dipolar and reversing dynamos (Kutzner and Christensen, 2002), although some special dynamos are dipole-dominated reversing (e.g. Olson 2007). Dipolarity and reversals define the "dynamo regime".
Studying numerical dynamos in a wide range of conditions, Christensen and Aubert (2006) discovered that the local Rossby number is a proxy of dynamo regime (see Fig. 1). Their finding has been confirmed by other works (Olson and Christensen, 2006; Aubert *et al.*, 2009; Driscoll and Olson, 2009) over a wider range of dynamo parameters. Aubert *et al.* (2009) found that dipolar dominated magnetic fields are generated by dynamos with values of Ro_l^* below a threshold of around 0.1. Driscoll and Olson (2009) have confirmed this result but using as a dipolarity proxy the modified Rayleigh number Ra_Q (see Figs. 2 and 3 in Driscoll and Olson (2009)). It should be stressed that although Ro_l^* could not be the only controlling factor of dipolarity, most of the available evidence points to this quantity as a good proxy for dynamo regime.
The value of Ro_l for the geodynamo is estimated at 0.08 (Olson and Christensen, 2006). For $\chi_\oplus = 0.35$ the value of $Ro_l^* = 0.07$. This places our planet close to the boundary between dipolar and multipolar dynamos. The reason the geodynamo is so close to that particular boundary is unknown (see section 6 for a discussion).
Dynamo regimes are thus separated in parameter space by complex boundaries broadly limited by approximate values of Ro_l^*. Non-reversing dipolar dynamos has $Ro_l^* < 0.04$ (irrespective of the type of convection and boundary conditions). The critical value of Ro_l^* for the transition from dipolar to multipolar regime is in the range $0.04 < Ro_l^* < 0.1$ depending for example of the type of convection. In numerical dynamo experiments, where several types of convection are considered, this region is populated by a mixture of non-reversing, reversing dynamos and multipolar dynamos. We denote this interval in Ro_l^* the "reversing region". Finally, dynamos with $Ro_l^* > 0.1$ are multipolar (see upper panel Fig. 1).

4. The role of rotation in the PMF properties

Using the results of the thermal evolution models and the scaling laws presented in section 3.1, we could try to constrain the expected properties of the PMF in SEs. Gaidos *et al.* (2010) and Tachinami *et al.* (2011) performed this task assuming rapidly rotating planets and hence dipolar dominated dynamos. This work go further by including the effect of rotation into determining the dynamo regime. This section will develop a general procedure to estimate the PMF properties in planets with dipolar and multipolar CMF, a condition required to estimate the magnetic properties of slowly rotating planets.

4.1. Rotation and CMF regime

In order to predict the evolution of CMF regime and to constrain the evolving PMF intensity, is necessary to find a general expression for the local Rossby number as a function of time, planetary mass and rotation rate. Replacing p as defined in Eq. (1) and using $E = \nu/(\Omega D^2)$, the scaling law for Ro_l^* in Eq. (5) can be written as:

$$Ro_l^* = c_{Rol} \times \left[Q_{conv}^{1/2} \Omega^{-3/2} D^{-1} (\overline{\rho}_c V)^{-1/2} \right] \times \left[\nu^{-1/3} \Omega^{1/3} D^{2/3} \right] \times (\lambda/\kappa)^{1/5} \tag{9}$$

In this expression Q_{conv} and $\chi = R_{ic}/R_c$ are provided directly by the thermal evolution model. Using χ is possible to compute $D = R_c(1-\chi)$ and $V = (4\pi/3)R_c^3(1-\chi^3)$. The core radius and average density are scaled using $R_c \propto M_p^{0.271}$ and $\overline{\rho}_c \propto M_p^{0.243}$ following Valencia *et al.* (2006). Finally, the rotation rate Ω is expressed in terms of the period of rotation P using $\Omega = 2\pi/P$ (see section 4.3 for further comments). The general expression for Ro_l^* as a function of time, mass and rotation is finally

$$Ro_l^*(t,M,P) = C\left[\overline{\rho}_c^{-1/6} R_c^{-11/6}\right] \times \left[Q_{conv}^{1/2}(1-\chi)^{-1/3}(1-\chi^3)^{-1/2}\right] \times P^{7/6} \quad (10)$$

Here we have separated the quantities that explicitly depend on planetary mass (first bracket) and those that depend explicitly on time and implicitly on mass (second bracket). The dependence on rotation has been isolated in the $P^{7/6}$ term. The quantity C depends on the core viscous, thermal and magnetic diffusivities that we will assume are nearly constant in time and almost independent of planetary mass. In our models C has been set imposing that a $1\,M_\oplus$ planet at $t = 4.54\ Gyr$ and $P = 1$ day has a value $Ro_l^*(t = 4.54\,Gyrs, M = 1\,M_\oplus, P = 1\,day) = 0.07$.
As can be seen in equation (10) the value of Ro_l^* strongly depends on the rotation period P. Slowly rotating dynamos (large P) will have large values of Ro_l^* and hence will be multipolar. It is also interesting to note that dynamos arising from a completely liquid iron core ($\chi = 0$) will have a smaller local Rossby number and hence will be dipolar dominated for a wider range of periods of rotation. In this case, however, in the absence of compositional convection the magnetic field strength could be much weaker. Additionally, for a fixed convective power, more massive planets will have smaller values Ro_l^* and they tend to have dipolar dominated dynamos.

4.2. Scaling the magnetic field intensity

Now the problem of estimating the CMF intensity in the dipolar and multipolar regimes is tackled starting from the thermal evolution model inputs Q_{conv} and $D = R_c(1-\chi)$ (see 3.1 for a D definition). Using the definition of b_{dip} (Eq. (8)) and the scaling law for B_{rms} (Eq. (6)) the dipolar field intensity at the CMB could be computed as,

$$\begin{aligned} \overline{B}_{dip} &= \frac{1}{b_{dip}} c_B f_{ohm}^{1/2} \sqrt{\overline{\rho}_c \mu_o}\, \Omega D p^{1/3} \\ &= \frac{1}{b_{dip}} c_B \sqrt{f_{ohm}\mu_o} \times \left[\overline{\rho}_c^{1/6} R_c^{-2/3}\right] \times \left[Q_{conv}^{1/3}(1-\chi)^{1/3}(1-\chi^3)^{-1/3}\right] \end{aligned} \quad (11)$$

Here the definition of p (Eq. (1)) was used and replaced D and V in terms of R_c and χ. It is customary to assume that in the case of rapid rotating dynamos $b_{dip} \sim 1$ and hence $\overline{B}_{dip} \sim B_{rms}$. That was the approximation used by Gaidos *et al.* (2010) and Tachinami *et al.* (2011) to estimate the field intensities reported in their works. However, in many relevant cases (see section 5.4) this approximation will not be valid and a proper prescription to estimate b_{dip} as a function of the thermal evolution model is required. We have studied the values of b_{dip} for a set of numerical dynamo results (Christensen and Aubert, 2006; Aubert *et al.*, 2009; Christensen, 2010; U.R. Christensen, personal communication, 2011) and found that although the value of this quantity varies in a wide range, both in the case of dipolar and multipolar dynamos, it is possible to find a lower bound b_{dip}^{min} that is a function of f_{dip} (see Fig. 1),

$$b_{dip}^{min} = c_{bdip} f_{dip}^{-\alpha}, \quad (12)$$

where $c_{bdip} \simeq 2.5$ and $\alpha \simeq 11/10$ are the best fitting parameters. Using this equation an upper bound to the dipolar field at the CMB could be computed directly from Eq. (11), replacing b_{dip} as b_{dip}^{min} from Eq. (12),

$$\overline{B}_{dip} \lesssim \overline{B}_{dip}^{max} = \frac{c_{Lo}}{c_{bdip}} f_{dip}^{11/10} \sqrt{f_{ohm}\mu_o} \times \left[\overline{\rho}_c^{1/6} R_c^{-2/3}\right] \times \left[Q_{conv}^{1/3}(1-\chi)^{1/3}(1-\chi^3)^{-1/3}\right] \quad (13)$$

The constant c_{Lo} adopts different values according to the dynamo regime: in the multipolar case ($f_{dip} \lesssim 0.35$), $c_{Lo} \simeq 1$ and in the dipolar case ($f_{dip} > 0.35$), $c_{Lo} \simeq 0.6$. Therefore, c_{Lo} depends implicitly on f_{dip}.
In summary, although f_{dip} and b_{dip} do not have unique values for dynamos in a given regime, they are constrained from above and below respectively, providing an interesting opportunity to constrain the dipolar component of the CMF. Estimating the local Rossby number of a planetary dynamo with a given rotation rate it is possible to compute the maximum value of f_{dip} attainable by dynamos at that Ro_l^* using numerical

dynamo results (upper panel in Fig. 1). With this quantity in hand and using equation (13) it is possible to calculate the maximum value of the dipolar component of the CMF.
It is possible to write down this procedure in the form of a simple algorithm. Given a planet with mass M_p and period of rotation P, the maximum dipolar component of the CMF at time t could be computed using the following procedure:

1. Using the thermal evolution model find $Q_{conv}(t)$ and $\chi(t)$.
2. Compute Ro_l^* using Eq. (10).
3. Using Ro_l^* compute the maximum value of f_{dip} as given by an envelop to numerical dynamo results in the $f_{dip} - Ro_l^*$ space (see dashed line in in the upper panel of Fig. 1).
4. Using f_{dip} compute the maximum dipolar component of the CMF, $\overline{B}_{dip}^{max}$ using Eq. (13). Values adopted for c_{Lo} are ≈ 1 for dipolar dynamos ($f_{dip} > 0.35$) and ≈ 0.6 for multipolar dynamos ($f_{dip} < 0.35$) (Aubert *et al.*, 2009; Christensen, 2010).

We are assuming $f_{ohm} \approx 1$ which is consistent with the goal to obtain an upper bound to the CMF.
Using the maximum intensity of the dipolar component of the CMF and assuming a low-conductivity mantle it is possible to estimate the magnetic field at the planetary surface. In the case of a dipolar dominated CMF the surface field intensity scales simply as $(R_c/R_p)^3$. But, if the CMF has a more complex power spectrum, the properties of the magnetic field at the surface are harder to estimate. However, since we are interested in the protective properties of the PMF and they mainly depend on the dipolar component of the field (Stadelmann *et al.*, 2010), we can still compute the maximum dipolar component of the PMF, $\overline{B}_{s,dip}^{max}$, using the formula:

$$\overline{B}_{s,dip}^{max} = \overline{B}_{dip}^{max} \left(\frac{R_c}{R_p} \right)^3 \tag{14}$$

Appendix A shows that this result is valid irrespective of dynamo regime.

4.3. Evolution of rotation rate

As was said in section 3.2, the dependence on rotation was expressed in terms of the period P instead of the rotation rate $\Omega = 2\pi/P$. P is better suited to study cases where rotation and orbital periods are related (tidal locking) or in cases where large tidal effects from planet-stellar interaction or due to hypothetical moons introduce simple long-term variation of P (Varga *et al.*, 1998).
The long-term evolution of rotation periods in terrestrial planets is a complex subject that depends on many different effects ranging from dynamical conditions at formation; catastrophic impacts; interior processes changing the distribution of matter to tidal interactions with the central star; close orbiting bodies or other bodies in the planetary system (see van Hoolts (2009) and references therein).
To model the long-term variations of the rotation period, it is necessary to considered two simple extreme scenarios: (1) Constant period of rotation P_o; this will be the case for tidally locked planets and also for planets that have preserved their primordial rotation, e.g. Mars. (2) Linearly increasing rotation period. This would be the case for planets affected by strong tidal damping from the central star, a close big moon or other planetary system bodies. In the latter scenario, and following the models used to study the long-term variation of the Earth's period of rotation (Varga *et al.*, 1998), we have assumed a simple linear variation,

$$P(t) = P_o + \dot{P}_o(t - t_o). \tag{15}$$

Here P_o and $\dot{P}_o$ are respectively the rotation period at t_o and its rate of variation. For an Earth-like rotation we assumed $t_o = 4.54$ Gyrs, $P_o = 24$ h and $\dot{P}_o \approx 1.5$ h Gyr^{-1}, values which are compatible with a primordial rotation of $P(t = 0) = P_{ini} \approx 17$ h (Varga *et al.*, 1998; Denis *et al.*, 2011).

5. Results

We have computed the evolution of Ro_l^* using Eq. (10) and the values of $Q_{conv}(t)$ and $\chi(t)$ provided by the CTE and MTE models in the cases highlighted in Table 2. The results for different planetary masses assuming P_o=24 h, both in the case of constant and variable period of rotation, are depicted in Fig. 2.
There are important differences between the results obtained with the CTE and the MTE models. These differences arise from the magnitude and evolution of the convective power density in both models (see Fig. 3). While in the CTE model the available power comes directly from the entropy dissipation inside the core, in the MTE model the amount of energy available for convection is simply bounded by the energy extracted by the mantle through the CMB. As a consequence, the power density is almost one order of magnitude larger and grows faster with planetary mass in the MTE case than in the CTE model. On the other hand, the energy flux through the CMB falls more rapidly in the MTE model than the entropy dissipated inside the core in the CTE model. This effect produces a net decrease in the power density at later times, at least in the case of low-mass SEs.
The most noticeable change in the evolution of the Ro_l^* happens during the so-called "p-rebound" just after the start of the inner core nucleation at time t_{ic}. In the CTE model, p goes through a sudden and strong increase at t_{ic} due to the combined effect of a convective power increase, which is the result of the release of latent heat and light elements, and the reduction in the vertical height D of the convecting shell. The p-rebound in the MTE model is milder and comes mainly from the reduction in D. In the MTE model the CMB flux F_{CMB} that determines the estimated value of Q_{conv}, is not sensitive to the new sources of entropy dissipation in the recently formed inner core. Although we are comparing both models in equivalent conditions, it is clear that the MTE model lacks very important details that reduce the likelihood of the conclusions drawn from the application of this model in our case.
Given these fundamental differences we will present separate analysis of the predicted properties of the CMF for the CTE and MTE models in the following paragraphs.

5.1. Role of rotation in the CTE model

The evolution of Ro_l^* for the CTE model is depicted in the upper panel of Fig. 2. As expected, the local Rossby number varies in time in a similar way as p does (see Fig. 3). Evolution of the period of rotation has an important effect, particularly when the convective power flux has dropped at late times.
In the case of low-mass planets, the p-rebound is responsible for the most important features of the Ro_l^* evolution. The sudden increase in p and the related decrease in D produce an even faster increase in Ro_l^*. This behavior has two effects: (1) Ro_l^* reaches a minimum value at t_{ic}, e.g. $Ro_{l,min}^* \simeq 0.02$ for $M = 1\,M_\oplus$ and $Ro_{l,min}^* \simeq 0.01$ for $M = 2\,M_\oplus$, regardless of variations in the period of rotation, and (2) the inner core nucleation, at certain periods of rotation (see below) will mark the transition from a dipolar to a multipolar regime.
In the case of massive planets where the solid inner core does not appear in the first 10 Gyrs, Ro_l^* steadily decreases until the dynamo finally shuts down. In this case the ability of the planet to create a dipolar CMF at large periods of rotation (slowly rotating planets) is constrained by the value of the local Rossby number close to the time of dynamo shut down. We found in this case that $Ro_{l,min}^* \sim 10^{-3}$, which is again independent of variations in the period of rotation.
Taking into account that $Ro_l^* \propto P^{7/6}$ (Eq. (10)) and using the critical value $Ro_l^* = 0.1$, at which all dynamos have became multipolar, we found that planets with a constant period of rotation $P \lesssim P_{mul} = P_o(0.1/Ro_{l,min}^*)^{6/7}$ will have a chance to develop a dipolar dominated CMF at some point in the dynamo lifetime. In the case of planets with $M \lesssim 2\,M_\oplus$ the limit is $P_{mul} \sim 4-9$ days (the lowest value corresponding to the lightest planet, 1 $M_\oplus$ and for more massive planets, i.e. $M \gtrsim 2\,M_\oplus$, $P_{mul} \sim 30-50$ days. These limits set upper bounds of what should be considered rapidly rotating planets, i.e. planets able to develop strong and long-lived dipolar magnetic fields. To find more precise limits it is necessary to compute the dipolar CMF lifetime, a problem that will be addressed below.
In order to understand the role of rotation in the survival of a dipolar dominated CMF in the case of planets with $M < 2\,M_\oplus$, the evolution of Ro_l^* must be studied for several values of the reference period of rotation P_o in the case of constant and variable rotation rate. The case for a $1\,M_\oplus$ planet with $P_o \approx 1.4$ days (33

h) is shown in Fig. 4. In this case the CMF dipolarity is guaranteed only during the first few Gyrs when no solid inner core has been formed and the convective power density is still down (low Ro_l^*). Shortly after the p-rebound the convective forces increase enough to make the CMF multipolar and the period of dipolar dominance ends. The time spent by the dynamo in the dipolar dominated regime is called the *dipolar lifetime*, T_{dip}. More massive SEs $M > 2\,M_\oplus$ exhibit a different behavior. For periods of rotation $P \lesssim P_{mul}$ the CMF is multipolar at the beginning and turns dipolar at a time called the dipolarity switch time, t_{sw}. In this case T_{dip} is computed as the difference between the dynamo lifetime and the t_{sw}.

A plot of T_{dip} for different planetary mass as a function of the reference period of rotation P_o is depicted in Fig. 5. As expected T_{dip} is equal to the dynamo lifetime in the case of rapidly rotating planets ($P_o \sim 1$ day). The critical period of rotation P_c up to which this condition is met, increases with planetary mass for $M \leq 2\,M_\oplus$ as a consequence of a later formation of the inner core in more massive planets (see Fig. 2). In the case of planets with $M > 2\,M_\oplus$, the critical period P_c is almost the same, $P_c \simeq 2 - 2.5$ days, a behavior explained by the similarity between the evolution of Ro_l^* in this type of planets (see upper panel in Fig. 2). A variable period of rotation decreases P_c for planets below $2\,M_\oplus$ but increases in the case of more massive planets. The explanation of this behavior could be found in the upper panel of Fig. 2. Low mass planets has a lower P_c if Ro_l^* is larger at late times and this is exactly the effect of a variable period of rotation. Conversely more massive planets has a larger P_c if Ro_l^* is lower at early times as expected again in the case of a variable period of rotation.

It is also interesting to note that in the case of low mass SEs, an intermediate level of dipolar CMF lifetime beyond P_c is found. This intermediate level is a by product of the steep increase in Ro_l^* around the time of inner core nucleation t_{ic}. For times $t < t_{ic}$ the dipolarity condition is ensured in a wide range of rotation rates. This effect explains why the dipolar lifetime at this intermediate level is close to t_{ic}. With these results it is possible to set a more stringent limit to the periods of rotation required to have long-lived ($T_{dip} \gtrsim 3$ Gyrs) dipolar dominated CMFs. We found that regardless of the mass, SEs with $P \lesssim 2 - 3$ days will meet this condition.

An interesting and nontrivial prediction arises from the dipolar lifetime dependence on mass and period. In the works by Gaidos *et al.* (2010) and Tachinami *et al.* (2011) low-mass planets were identified as the best candidates to have intense, long-lived PMF. This result was a consequence of the favorable conditions that the early nucleation of a solid inner core and a lower viscosity mantle have on the determination of the PMF properties and its lifetime. This result is still valid here, at least for planets with periods of rotation smaller than ~ 1.5 days. However, when rotation periods are larger than this limit the roles are interchanged: massive Super Earths would develop a dipolar CMF for a longer time than the lightest planets. The reason for this switch is the strong p-rebound when the inner core starts to nucleate in light SEs. Since the thermal evolution of massive planets does not exhibit such rebound, the rotation period for $M > 2\,M_\oplus$ could be increased even more, before the CMF becomes multipolar.

Taking into account the evolution of Ro_l^* and the information it could provide on the CMF regime, we have computed the intensity of the dipolar component of the PMF, $\overline{B}_{s,dip}$ following the procedure outlined in section 4.2. The result is depicted in Fig. 6 where we have additionally included the measured value of the Earth magnetic field at present times (Maus *et al.*, 2005) and three recent measured paleomagnetic intensities at 3.2 and 3.4 Gyrs ago (Tarduno *et al.*, 2010) (indicated with an Earth symbol and error bars respectively). It is clear in this case that the evolution of the Ro_l^* has an important impact on the measured field at the planetary surface. In the case of an Earth mass planet with $P = 1.5$ days (lower panel in Fig. 6) the dipolar component of the field reaches a maximum intensity almost 300 Myrs after the initiation of the inner core nucleation just to decay again in hundreds of megayears as a consequence of the increase in intensity of the convective currents vs. the weak Coriolis force. At 3 Gyrs the CMF becomes fully multipolar and the intensity measured at the surface is just the CMF dipolar component. We have assumed that the transition from the dipolar to the multipolar regime happens in short times when compared with the thermal evolution time scales.

In order to compare the dipolar PMF intensities of planets with different masses and to understand the global role of rotation in the determination of the PMF properties, the dipolar field intensity averaged over the dynamo lifetime T_{dyn} was computed

$$B_{avg} \equiv < \overline{B}_{s,dip} >= T_{dyn}^{-1} \int_0^{T_{dyn}} \overline{B}_{s,dip} dt \quad (16)$$

Although not phenomenologically relevant this quantity is very useful to compare the PMF for evolving dynamos with different planetary parameters. On the other hand the minimum and maximum "historical" dipolar field intensities for a given planetary mass and rotation rate, observed in a relevant range of parameters, are of the same order of this average and therefore B_{avg} seems a good first order estimate of the evolving PMF intensity. In Fig. 7 we plot B_{avg} vs. P_o for planets with different masses. We found a similar behavior of B_{avg} as that found in T_{dip} (Fig. 5). In this case however the differences between the field intensities are not as noticeable as those found in the case of the dipolar CMF lifetime.

Field intensity is not the only observable we can try to estimate with this model. Reversal frequencies could also be inferred (Driscoll and Olson, 2009). Although we have not computed this property it should be mentioned that the predicted monotonous variation of the local Rossby number could not explain completely the variation in reversal frequency observed in the Earth's paleomagnetic field. For example the increase in Ro_l^* after inner core nucleation could explain the transition from a superchrone to reversals but not from reversals to superchrone.

Displaying the properties of an evolving magnetic field (dipolar lifetime and intensity) for different planetary masses and periods of rotation is challenging. To simplify the graphical representation of PMF properties and their dependence on mass and rotation rate, we introduce here the Mass-Period diagram (hereafter *M-P* diagram). We have used *M-P* diagrams in Fig. 8 to depict T_{dip} and B_{avg} for the CTE model, comparing the cases of constant and variable periods of rotation. The conclusions drawn from Figs. 5 and 7 are well illustrated in the *M-P* diagrams (see Fig. 8). Planets with masses between 1 and 3 $M_\oplus$ and periods $P < 3$ days, are the best suited to developing a long-lived dipolar field, and planets with $M < 2\,M_\oplus$ and $P < 1.5$ days develop dipolar field intensities of the same order as the Earth's. Qualitatively the effects of a variable period of rotation are negligible.

5.2. Role of rotation in the MTE model

The evolution of Ro_l^* for the MTE model is plotted in the lower panel of Fig. 2. In all the cases the Ro_l^* has large values at early times and hence the predicted CMF is always multipolar at the beginning. This result is a consequence of the large initial CMB flux F_{CMB} used in this model to estimate the convective power at the core. For all the planetary masses and in the case of rapidly rotating planets, dynamos switch from a multipolar to a dipolar regime at what we have called the dipolar switch time t_{sw}. In several cases, the intensity of the *p*-rebound and/or the variation of the period of rotation reduce the time spent for the dynamo in a dipolar dominated state T_{dip}. In the analogous to Fig. 8 for the CTE model, we have plotted t_{sw} and T_{dip} in *M-P* diagrams in Fig. 9. In order to have a protective PMF it is expected that the core CMF becomes dipolar as early as possible (small t_{sw}). Indeed a protective PMF is more important in the early phases of planetary and stellar evolution evolution than at late times (see e.g. Lichtenegger *et al.* 2010). We also expect that the duration of the dipolarity phase T_{dip} be also large. The effects of a variable period of rotation are noticeable especially in the case of large mass planets. This fact is the result of the particular behavior of the evolving Ro_l^*.

For the MTE model the limit for rapidly rotating planets, as estimated by the condition to have long-lived dipolar fields, is more stringent than in the CTE model. Only planets with periods shorter than 1 day develop intense and long lived dipolar CMF in contrast with approximately 2-3 days limit found in the case of the CTE model.

5.3. Rotation based SEs classification

The resulting effects that a variation in the rotation period has in the dynamo properties of SEs, suggest the possibility to classify SE dynamos in three different groups: rapid, slow and very slow rotators (see Fig. 5). **Rapid rotators** are planets with strong dipolar dominated dynamos lasting several to tens of Gyrs. This type of planets have dynamos with local Rossby numbers below the critical value, i.e. operating in the dipolar regime, for the most part of the dynamo lifetime (50% is the criterion used here). Our planet

would belong to this group. **Slow rotators** are SEs with dipolar dynamos lasting for less than 50% of the dynamo lifetime. Dynamos of this type spends most time of their lifetime in the reversing region and a non negligible time above the critical value for the multipolar regime. **Very slow rotators** correspond to planets that do not develop a dipolar dominated field during their entire dynamo lifetime. Dynamos of this type have large super critical local Rossby numbers.
The range of periods of rotation defining the proposed categories, varies with mass and depends on the particular thermal evolution model used to predict the PMF properties. In the case of the CTE model we found that rapid rotators have $P \lesssim 1.5$ days, irrespective of planetary mass, slow rotators with masses $M \lesssim 2\,M_{\oplus}$ have periods of rotation in the range $4 \lesssim P \lesssim 10$ days, while more massive slow rotators will have $4 \lesssim P \lesssim 20$ days. Planets with $P \gtrsim 10 - 20$ days are very slow rotators. We have plotted these limits in Fig. 5. In the case of the MTE model the limit for rapid rotators are more stringent than in the CTE model. This fact is a consequence of the high convective power predicted by this model at early times (see lower panel in Figs. 2 and 3). The maximum rotation rate for rapid rotating planets in this case is not larger than 1 day. The category of slow rotators is practically nonexistence in this model. Planets with periods of rotation larger than $1 - 1.5$ days will be very slow rotators if the thermal evolution model has the features predicted by the MTE model.

5.4. Application to already discovered SEs

The application of these results to study the development of protective magnetic fields in newly discovered SEs, depends on the ability to know or estimate their rotation periods. The most of already discovered SEs are tidally locked and hence their rotation periods are also known. According to recent claims, planets with masses in the range of interest for this work ($M < 2\,M_{\oplus}$) and orbital periods less than 50 days could be common around low-mass stars (Howard *et al.*, 2010). Therefore, tidally locked SEs are the best initial target for this kind of analysis. Nevertheless, in the case of unlocked SEs yet to be discovered the feasibility to measure the period of rotation using present and future observational facilities has also been devised (see Ford *et al.* (2001) and Pallé *et al.* (2008) and references therein).
In Fig. 10 we have plotted the habitable zone (HZ) for GKM stars and the physical parameters of confirmed SEs plus the subset of Kepler candidates inside the HZ (Borucki *et al.*, 2011). We have also included there, contours of equilibrium temperatures (Selsis *et al.*, 2007; Lammer *et al.*, 2010), the outer limits to have tidally locked planets in 1 and 3 Gyrs (Kasting *et al.*, 1993), and the range of periods defining our categories of rapid, slow and very slow rotators in the case of massive SEs assuming the CTE thermal evolution model. It is needed to point out that the results have a limited range of applicability when compared with the wide range of physical properties founded in this set of discovered SEs. We have assumed from the beginning that planets have a composition similar to Earth, habitable temperatures and mobile lids. Low density planets as GJ 1214b probably covered by thick volatile atmospheres (Nettelmann *et al.*, 2011), could have other ways to create intrinsic magnetic fields and the limits to develop protective PMF should be different than those found here in the case of core dynamos. Nevertheless, rotation will still play an interesting role in the PMF properties of these types of planets and efforts to include this effect should not be underestimated. On the other hand the composition of many of these SEs is still unknown (there is a lack of complete information on their masses and radii). SEs with high surface temperatures, e.g. Corot 7b (Valencia *et al.*, 2010), also fall outside the range of applicability of these results. Higher surface temperatures reduce the viscosity in the mantle favoring the extraction of energy from the core and increasing the convective power energy. Gaidos *et al.* (2010) found higher values of the surface PMF in the case of $\approx O(1)M_{\oplus}$ planets and larger dynamos lifetime in more massive SEs, when surface temperatures are increased. In those cases the Ro_l^* will also be larger and the critical period of rotation to have multipolar dynamos will be smaller. These results suggest that hot SEs would lack of protective magnetic fields even with periods of rotation proper of colder slow rotators.

6. Discussion

This work relies basically on three hypotheses: (1) the thermal evolution models by Gaidos *et al.* (2010) and Tachinami *et al.* (2011) provide global robust features of the thermal evolution in SEs, (2) The scaling laws

fitted with numerical dynamo experiments can be extrapolated to regions in the parameter space where real planetary dynamos lie, (3) the local Rossby number could be used as a proxy for dynamo regime.

It is clear that to test hypothesis (1) it is necessary to address the open questions left by Gaidos *et al.* (2010) and Tachinami *et al.* (2011). It is important to solve a complete model including a rigorous treatment of convection in the mantle, as was done in the MTE model, but also taking into account a detailed model of the structure and entropy balance in the core as done by the CTE model. Despite the limitations, there are two robust predictions from these models that may be confirmed by more complete models or even by observations: (1) there is a maximum planetary mass, $\sim 2\,M_{\oplus}$ beyond which conditions to develop strong and long-lived PMF decline; (2) the formation of a solid inner core is favored in the case of $\approx O(1)M_{\oplus}$ planets. These two features are of fundamental importance to our results. Changes in other outputs of the thermal evolution model such as the differences between the convective power for planets with different mass or the role that other planetary properties will have in the onset of a dynamo, will not change the conclusions of this work.

Hypothesis (2) is also a matter of concern in present studies of planetary and stellar dynamos (Christensen, 2010). Although the application of numerical dynamo-based scaling laws to planetary dynamos has had some success (Olson and Christensen, 2006), higher resolution in future numerical experiments aimed at exploring a wider region of the parameter space is required to confirm this hypothesis. Further advances in the understanding of how non dipolar dynamos behave will also be required to support the procedure devised in this work to estimate the PMF intensity in that case.

Hypothesis (3) relies again on inferences from extensive numerical dynamo experiments (see Fig. 1). Since the numerical parametric studies of Sreenivasan and Jones (2006) it is well known that dipolarity decreases with the increase of the ratio of inertial to Coriolis forces. Christensen and Aubert (2006) identified a critical value for Ro_l^*, this critical behavior has been confirmed by more recent studies performed by Aubert *et al.* (2009), Driscoll and Olson (2009) and Christensen (2010). Driscoll and Olson (2009) found a threshold in Ra_Q separating the dipolar and multipolar regimes (see Fig. 3b in their paper) consistent with the Ro_l^* critical value found by Christensen and Aubert (2006) and Aubert *et al.* (2009). Less clear are the properties of the dynamos lying close to the boundary between the dipolar and multipolar regimes. The best known planetary dynamo, i.e. the Earth's dynamo, is just right there. Driscoll and Olson (2009) discussed the relationship between the particular reversal history of the Earth and the unknown properties of the transitional region between dipolar and multipolar regimes in parametric space. In this case however an open question remains: why is the Earth's dynamo so close to this boundary? The scaling law for Ro_l^* found in Eq. (10) could shed light into this "coincidence problem". It is noted that the particular thermal history of our planet does not affect to a large extent the order of magnitude of Ro_l^*. As shown in Fig. 2 and 3, one or two orders of magnitude variation of p are not enough to change the order of magnitude of Ro_l^*. This quantity is more sensitive to the period of rotation and the core radius of the planet. The period of rotation of the Earth has been of the same order since the formation of the planet (Denis *et al.*, 2011) and it is close to that of Mars. The core radius is mainly determined by the Fe/Si ratio, a quantity that is not "fine-tuned" for the Earth since Venus and Mars has a similar value of this ratio. In conclusion the present value of the Earth's dynamo local Rossby number is not just coincidentially close to the boundary region since, as argued here, reasonable variations in the key properties of the dynamo will place it not too far from this region.

It should be stressed that after the results presented in this work and taking into account the fact that probably most of the habitable SEs lie in tidally locked regions (see e.g. Boss 2006 and Forveille *et al.* 2009) where large periods of rotation could be common, future efforts to try to understand the emergence and evolution of PMFs in these types of planets, must consider the kind of direct and indirect effects that rotation have in the PMF properties as those considered here. In other words the assumption of rapidly rotating planets, i.e. $P \lesssim 2$ days, is no longer valid if we want to study tidally locked SEs inside the HZ of M-dwarfs. On the other hand assuming that tidally locked planets lacks completely of an intense planetary magnetic field is also an oversimplification. As has been shown here there are a range of periods of rotation where planets could sustain moderate magnetic fields having large periods of rotation.

Thermal evolution models used in this work assumed planetary properties very similar to Earth. Gaidos *et al.* (2010) studied the impact that several modifications to this reference model will have on their results. An

interesting case is that of planets with a different relative core size. They found that an increase in core size (a larger Fe to Si ratio) essentially has two effects: (1) an earlier nucleation of the solid inner core and (2) an increase of the surface magnetic field intensity. The latter effect is mostly due to the smaller attenuation of core field and not to a noticeable modification of the convective power density. A different core size changes our results in two important ways: (1) the predicted maximum dipolar component of the PMF is increased and (2) the dipolar field lifetime, especially in the case of slow rotators, is decreased. Assuming that a different core size does not affect noticeably the convective power, the local Rossby number will be slightly modified and hence the general results regarding, for example, the intervals of rotation periods for the new categories of rotators, will not be substantially altered.

7. Summary and conclusions

We studied the role of rotation in the evolution of dynamo-generated magnetic fields in Super Earths. We computed the evolution of the local Rossby number and the volumetric magnetic field strength for core dynamos in SEs. For this purpose we used the results of two recently published thermal evolution models and scaling laws fitted with numerical dynamo experiments. Assuming that the local Rossby number could be used as a proxy to dynamo regime, we estimated the maximum dipolar component of the magnetic field at the CMB, and from it an upper bound to the dipolar part of the field at the planetary surface.

We used two properties to characterize the global magnetic properties of SEs: (1) the average of the surface dipolar component of the field, B_{avg} and (2) the total time T_{dip} spent by the dynamo in the dipolar dominated regime (reversing and non reversing). Intense magnetic fields with a strong dipolar component (Stadelmann *et al.*, 2010), are best suited to protect planetary environments from external agents (stellar wind and cosmic rays). Therefore large values of B_{avg}, irrespective of the dynamo regime, are consistent with planetary habitability. The long-term preservation of water and other volatiles in a planetary atmosphere and the development of life, would require long-lived protective PMFs, i.e. large values of T_{dip}. Intense and protective magnetic fields in the early phases of planetary and stellar evolution will be also suited for the preservation of an atmosphere or its volatiles. However a planet that achieves to preserve its atmosphere during the harsh conditions of the early active phases of stellar evolution but lacks of a protective magnetic field soon after this period will leave emerging forms of life to an integrated effect of galactic and stellar cosmic rays induced damages.

We found that the PMF properties depend strongly on planetary mass and rotation period. Rapidly rotating SEs $P \approx O(1)$ day, with mass $\approx O(1)\, M_{\oplus}$, have the best potential to develop long-lived and intense PMFs. More massive planets develop weaker magnetic fields but they have dipolar dominated dynamos in a slightly larger range of rotational periods $P \sim 1 - 3$ days. SEs with rotation periods larger than $3 - 10$ days (depending on their mass) will spend the majority of the dynamo lifetime in a multipolar state.

In order to summarize our results we have introduced a rotation-based classification. Using the CTE thermal evolution model, SEs could be rapid rotators $P \lesssim 1.5 - 4$ days, slow rotators $4 \lesssim P \lesssim 10 - 20$ days and otherwise, very slow rotators. Planets in the HZ of low mass stars $M_{\star} < 0.6$ that will be tidally locked in less than 1 Gyr, will fall between the slow and very slow rotator types. Unlocked planets could be any of the types described before, according to their primordial period of rotation and the effects that could dampen it.

More theoretical and observational efforts should be undertaken to address the problem of direct or indirect detection of PMF around low mass planets. The detection and measurement of such planetary magnetic fields will help us to constrain thermal evolution and dynamo models. The role of magnetic fields in planetary habitability is another problem that deserves close attention. Recent works have tackled this problem in detail (Grießmeier *et al.*, 2010) but their PMF models are too simplistic. Although the effect of rotation rates is considered in those models and they have focused on tidally locked planets, their models do not include the effects of thermal evolution on the PMF properties and their treatment of the dependence of these properties of the rotation rate is also limited.

Acknowledgments

We want to thank D. Valencia for encouraging us to complete this work and for her useful comments and discussion about our first approximations of the problem. We also thank S. Labrosse and U.R. Christensen for their kind answers to our questions on numerical dynamo experiments and thermal evolution of the Earth's core. Special thanks to E. Gaidos who kindly provided us with details of the results published in Gaidos *et al.* (2010). U.R. Christensen kindly shared with us the results of tens of numerical dynamo experiments that were fundamental to improve our results and to confirm our conclusions. We are also grateful with Luz Angela Cubides and Luke Webb for the final revision of the manuscript. Finally we thank the anonymous referees who made so many useful comments on the content and about the style of the manuscript which at the end led to its final form. PC is supported by the Vicerrectoria de Docencia of the Universidad de Antioquia. This work has been done with the financial support of the CODI-UdeA under Project IN591CE and the Universidad de Medellin under the Project CIDI479.

References

Adams, E. R., S. Seager, and L. Elkins-Tanton 2008. Ocean Planet or Thick Atmosphere: On the Mass-Radius Relationship for Solid Exoplanets with Massive Atmospheres. *ApJ* **673**, 1160–1164.

Amit, H., R. Leonhardt, and J. Wicht 2010. Polarity Reversals from Paleomagnetic Observations and Numerical Dynamo Simulations. *Space Sci. Rev.* **155**, 293–335.

Aubert, J., S. Labrosse, and C. Poitou 2009. Modelling the palaeo-evolution of the geodynamo. *Geophysical Journal International* **179**, 1414–1428.

Backus, G., Parker, R.L., and C. Constable 1996. *Foundations of Geomagnetism.*

Baraffe, I., G. Chabrier, and T. Barman 2008. Structure and evolution of super-Earth to super-Jupiter exoplanets. I. Heavy element enrichment in the interior. *A&A* **482**, 315–332.

Beaulieu, J.-P., D. P. Bennett, P. Fouqué, A. Williams, M. Dominik, U. G. Jørgensen, D. Kubas, A. Cassan, C. Coutures, J. Greenhill, K. Hill, J. Menzies, P. D. Sackett, M. Albrow, S. Brillant, J. A. R. Caldwell, J. J. Calitz, K. H. Cook, E. Corrales, M. Desort, S. Dieters, D. Dominis, J. Donatowicz, M. Hoffman, S. Kane, J.-B. Marquette, R. Martin, P. Meintjes, K. Pollard, K. Sahu, C. Vinter, J. Wambsganss, K. Woller, K. Horne, I. Steele, D. M. Bramich, M. Burgdorf, C. Snodgrass, M. Bode, A. Udalski, M. K. Szymański, M. Kubiak, T. Więckowski, G. Pietrzyński, I. Soszyński, O. Szewczyk, Ł. Wyrzykowski, B. Paczyński, F. Abe, I. A. Bond, T. R. Britton, A. C. Gilmore, J. B. Hearnshaw, Y. Itow, K. Kamiya, P. M. Kilmartin, A. V. Korpela, K. Masuda, Y. Matsubara, M. Motomura, Y. Muraki, S. Nakamura, C. Okada, K. Ohnishi, N. J. Rattenbury, T. Sako, S. Sato, M. Sasaki, T. Sekiguchi, D. J. Sullivan, P. J. Tristram, P. C. M. Yock, and T. Yoshioka 2006. Discovery of a cool planet of 5.5 Earth masses through gravitational microlensing. *Nature* **439**, 437–440.

Bonfils, X., M. Gillon, T. Forveille, X. Delfosse, D. Deming, B.-O. Demory, C. Lovis, M. Mayor, V. Neves, C. Perrier, N. C. Santos, S. Seager, S. Udry, I. Boisse, and M. Bonnefoy 2011. A short-period super-Earth orbiting the M2.5 dwarf GJ 3634. Detection with HARPS velocimetry and transit search with Spitzer photometry. *A&A* **528**, A111.

Borucki, W. J., D. G. Koch, G. Basri, N. Batalha, A. Boss, T. M. Brown, D. Caldwell, J. Christensen-Dalsgaard, W. D. Cochran, E. DeVore, E. W. Dunham, A. K. Dupree, T. N. Gautier, III, J. C. Geary, R. Gilliland, A. Gould, S. B. Howell, J. M. Jenkins, H. Kjeldsen, D. W. Latham, J. J. Lissauer, G. W. Marcy, D. G. Monet, D. Sasselov, J. Tarter, D. Charbonneau, L. Doyle, E. B. Ford, J. Fortney, M. J. Holman, S. Seager, J. H. Steffen, W. F. Welsh, C. Allen, S. T. Bryson, L. Buchhave, H. Chandrasekaran, J. L. Christiansen, D. Ciardi, B. D. Clarke, J. L. Dotson, M. Endl, D. Fischer, F. Fressin, M. Haas, E. Horch, A. Howard, H. Isaacson, J. Kolodziejczak, J. Li, P. MacQueen, S. Meibom, A. Prsa, E. V. Quintana, J. Rowe, W. Sherry, P. Tenenbaum, G. Torres, J. D. Twicken, J. Van Cleve, L. Walkowicz, and H. Wu 2011. Characteristics of Kepler Planetary Candidates Based on the First Data Set. *ApJ* **728**, 117.

Boss, A. P. 2006. Rapid Formation of Super-Earths around M Dwarf Stars. *ApJL* **644**, L79–L82.

Breuer, D., S. Labrosse, and T. Spohn 2010. Thermal Evolution and Magnetic Field Generation in Terrestrial Planets and Satellites. *Space Sci. Rev.* **152**, 449–500.

Christensen, U. R. 2010. Dynamo Scaling Laws and Applications to the Planets. *Space Sci. Rev.* **152**, 565–590.

Christensen, U. R., and J. Aubert 2006. Scaling properties of convection-driven dynamos in rotating spherical shells and application to planetary magnetic fields. *Geophysical Journal International* **166**, 97–114.

Christensen, U. R., V. Holzwarth, and A. Reiners 2009. Energy flux determines magnetic field strength of planets and stars. *Nature* **457**, 167–169.

Denis, C., K. R. Rybicki, A. A. Schreider, S. Tomecka-Suchoń, and P. Varga 2011. Length of the day and evolution of the Earth's core in the geological past. *Astronomische Nachrichten* **332**, 24–35.

Driscoll, P., and P. Olson 2009. Effects of buoyancy and rotation on the polarity reversal frequency of gravitationally driven numerical dynamos. *Geophysical Journal International* **178**, 1337–1350.

Driscoll, P., and P. Olson 2011. Optimal dynamos in the cores of terrestrial exoplanets: Magnetic field generation and detectability. *Icarus* **213**, 12–23.

Ford, E. B., S. Seager, and E. L. Turner 2001. Characterization of extrasolar terrestrial planets from diurnal photometric variability. *Nature* **412**, 885–887.

Fortney, J. J., M. S. Marley, and J. W. Barnes 2007. Planetary Radii across Five Orders of Magnitude in Mass and Stellar Insolation: Application to Transits. *ApJ* **659**, 1661–1672.

Forveille, T., X. Bonfils, X. Delfosse, M. Gillon, S. Udry, F. Bouchy, C. Lovis, M. Mayor, F. Pepe, C. Perrier, D. Queloz, N. Santos, and J.-L. Bertaux 2009. The HARPS search for southern extra-solar planets. XIV. Gl 176b, a super-Earth rather than a Neptune, and at a different period. *A&A* **493**, 645–650.

Gaidos, E., C. P. Conrad, M. Manga, and J. Hernlund 2010. Thermodynamic Limits on Magnetodynamos in Rocky Exoplanets. *ApJ* **718**, 596–609.

Grasset, O., J. Schneider, and C. Sotin 2009. A Study of the Accuracy of Mass-Radius Relationships for Silicate-Rich and Ice-Rich Planets up to 100 Earth Masses. *ApJ* **693**, 722–733.

Grießmeier, J.-M., M. Khodachenko, H. Lammer, J. L. Grenfell, A. Stadelmann, and U. Motschmann 2010. Stellar activity and magnetic shielding. In A. G. Kosovichev, A. H. Andrei, & J.-P. Roelot (Ed.), *IAU Symposium*, Volume 264 of *IAU Symposium*, pp. 385–394.

Grießmeier, J.-M., A. Stadelmann, J. L. Grenfell, H. Lammer, and U. Motschmann 2009. On the protection of extrasolar Earth-like planets around K/M stars against galactic cosmic rays. *Icarus* **199**, 526–535.

Grießmeier, J.-M., A. Stadelmann, U. Motschmann, N. K. Belisheva, H. Lammer, and H. K. Biernat 2005. Cosmic Ray Impact on Extrasolar Earth-Like Planets in Close-in Habitable Zones. *Astrobiology* **5**, 587–603.

Howard, A. W., G. W. Marcy, J. A. Johnson, D. A. Fischer, J. T. Wright, H. Isaacson, J. A. Valenti, J. Anderson, D. N. C. Lin, and S. Ida 2010. The Occurrence and Mass Distribution of Close-in Super-Earths, Neptunes, and Jupiters. *Science* **330**, 653–655.

Kaltenegger, L. 2010. Characterizing Habitable Exomoons. *ApJL* **712**, L125–L130.

Kaltenegger, L., W. G. Henning, and D. D. Sasselov 2010. Detecting Volcanism on Extrasolar Planets. *AJ* **140**, 1370–1380.

Kasting, J. F., D. P. Whitmire, and R. T. Reynolds 1993. Habitable Zones around Main Sequence Stars. *Icarus* **101**, 108–128.

Korenaga, J. 2010. On the Likelihood of Plate Tectonics on Super-Earths: Does Size Matter? *ApJL* **725**, L43–L46.

Kutzner, C., and U. R. Christensen 2002. From stable dipolar towards reversing numerical dynamos. *Physics of the Earth and Planetary Interiors* **131**, 29–45.

Labrosse, S. 2003. Thermal and magnetic evolution of the Earth's core. *Physics of the Earth and Planetary Interiors* **140**, 127–143.

Labrosse, S. 2007a. *Encyclopedia of Geomagnetism and Paleomagnetism*, Chapter Heat flow across the core-mantle boundary, pp. 127–130. Springer.

Labrosse, S. 2007b. *Encyclopedia of Geomagnetism and Paleomagnetism*, Chapter Energy sources for the geodynamo, pp. 300–308. Springer.

Lammer, H., F. Selsis, E. Chassefière, D. Breuer, J.-M. Grießmeier, Y. N. Kulikov, N. V. Erkaev, M. L. Khodachenko, H. K. Biernat, F. Leblanc, E. Kallio, R. Lundin, F. Westall, S. J. Bauer, C. Beichman, W. Danchi, C. Eiroa, M. Fridlund, H. Gröller, A. Hanslmeier, W. Hausleitner, T. Henning, T. Herbst, L. Kaltenegger, A. Léger, M. Leitzinger, H. I. M. Lichtenegger, R. Liseau, J. Lunine, U. Motschmann, P. Odert, F. Paresce, J. Parnell, A. Penny, A. Quirrenbach, H. Rauer, H. Röttgering, J. Schneider, T. Spohn, A. Stadelmann, G. Stangl, D. Stam, G. Tinetti, and G. J. White 2010. Geophysical and Atmospheric Evolution of Habitable Planets. *Astrobiology* **10**, 45–68.

Lichtenegger, H. I. M., H. Lammer, J.-M. Grießmeier, Y. N. Kulikov, P. von Paris, W. Hausleitner, S. Krauss, and H. Rauer 2010. Aeronomical evidence for higher CO_2 levels during Earth's Hadean epoch. *Icarus* **210**, 1–7.

Lissauer, J. J., D. C. Fabrycky, E. B. Ford, W. J. Borucki, F. Fressin, G. W. Marcy, J. A. Orosz, J. F. Rowe, G. Torres, W. F. Welsh, N. M. Batalha, S. T. Bryson, L. A. Buchhave, D. A. Caldwell, J. A. Carter, D. Charbonneau, J. L. Christiansen, W. D. Cochran, J.-M. Desert, E. W. Dunham, M. N. Fanelli, J. J. Fortney, T. N. Gautier, III, J. C. Geary, R. L. Gilliland, M. R. Haas, J. R. Hall, M. J. Holman, D. G. Koch, D. W. Latham, E. Lopez, S. McCauliff, N. Miller, R. C. Morehead, E. V. Quintana, D. Ragozzine, D. Sasselov, D. R. Short, and J. H. Steffen 2011. A closely packed system of low-mass, low-density planets transiting Kepler-11. *Nature* **470**, 53–58.

Lister, J. R. 2003. Expressions for the dissipation driven by convection in the Earth's core. *Physics of the Earth and Planetary Interiors* **140**, 145–158.

Maus, S., H. Lühr, G. Balasis, M. Rother, and M. Mandea 2005. *Earth Observation with CHAMP Results from Three Years in Orbit*, Chapter Introducing POMME, the POtsdam Magnetic Model of the Earth, pp. 293–298. Springer.

Mayor, M., and S. Udry 2008. The quest for very low-mass planets. *Physica Scripta Volume T 130*(1), 014010+08.

Nettelmann, N., J. J. Fortney, U. Kramm, and R. Redmer 2011. Thermal Evolution and Structure Models of the Transiting Super-Earth GJ 1214b. *ApJ* **733**, 2–13.

Nimmo, F. 2009. *Treatise on Geophysics*, Volume 8, Chapter Enegetics of the Core, pp. 31–68. Elsevier.

Olson, P. 2007. Gravitational dynamos and the low-frequency geomagnetic secular variation. In T. N. A. of Sciences of the USA (Ed.), *Proceedings of the National Academy of Sciences*, Volume 104, pp. 2015920166.

Olson, P. 2007. Overview. In G. Schubert (Ed.), *Treatise on Geophysics: Volume 8, Core dynamics*, pp. 1–30. Elsevier B.V.

Olson, P., and U. R. Christensen 2006. Dipole moment scaling for convection-driven planetary dynamos. *Earth and Planetary Science Letters* **250**, 561–571.

Pallé, E., E. B. Ford, S. Seager, P. Montañés-Rodríguez, and M. Vazquez 2008. Identifying the Rotation Rate and the Presence of Dynamic Weather on Extrasolar Earth-like Planets from Photometric Observations. *ApJ* **676**, 1319–1329.

Papuc, A. M., and G. F. Davies 2008. The internal activity and thermal evolution of Earth-like planets. *Icarus* **195**, 447–458.

Queloz, D., F. Bouchy, C. Moutou, A. Hatzes, G. Hébrard, R. Alonso, M. Auvergne, A. Baglin, M. Barbieri, P. Barge, W. Benz, P. Bordé, H. J. Deeg, M. Deleuil, R. Dvorak, A. Erikson, S. Ferraz Mello, M. Fridlund, D. Gandolfi, M. Gillon, E. Guenther, T. Guillot, L. Jorda, M. Hartmann, H. Lammer, A. Léger, A. Llebaria, C. Lovis, P. Magain, M. Mayor, T. Mazeh, M. Ollivier, M. Pätzold, F. Pepe, H. Rauer, D. Rouan, J. Schneider, D. Segransan, S. Udry, and G. Wuchterl

2009. The CoRoT-7 planetary system: two orbiting super-Earths. *A&A* **506**, 303–319.
Ribas, I., A. Font-Ribera, and J.-P. Beaulieu 2008. A ˜5 $M_\oplus$ Super-Earth Orbiting GJ 436? The Power of Near-Grazing Transits. *ApJL* **677**, L59–L62.
Rivera, E. J., J. J. Lissauer, R. P. Butler, G. W. Marcy, S. S. Vogt, D. A. Fischer, T. M. Brown, G. Laughlin, and G. W. Henry 2005. A ˜7.5 $M_\oplus$ Planet Orbiting the Nearby Star, GJ 876. *ApJ* **634**, 625–640.
Roberts, P. H., and G. A. Glatzmaier 2000. Geodynamo theory and simulations. *Reviews of Modern Physics* **72**, 1081–1123.
Seager, S., M. Kuchner, C. A. Hier-Majumder, and B. Militzer 2007. Mass-Radius Relationships for Solid Exoplanets. *ApJ* **669**, 1279–1297.
Selsis, F., J. F. Kasting, B. Levrard, J. Paillet, I. Ribas, and X. Delfosse 2007. Habitable planets around the star Gliese 581? *A&A* **476**, 1373–1387.
Sotin, C., O. Grasset, and A. Mocquet 2007. Mass-radius curve for extrasolar Earth-like planets and ocean planets. *Icarus* **191**, 337–351.
Sreenivasan, B., and C. A. Jones 2006. The role of inertia in the evolution of spherical dynamos. *Geophysical Journal International* **164**, 467–476.
Stadelmann, A., J. Vogt, K.-H. Glassmeier, M.-B. Kallenrode, and G.-H. Voigt 2010. Cosmic ray and solar energetic particle flux in paleomagnetospheres. *Earth, Planets, and Space* **62**, 333–345.
Stevenson, D. J. 2003. Planetary magnetic fields. *Earth and Planetary Science Letters* **208**, 1–11.
Tachinami, C., H. Senshu, and S. Ida 2011. Thermal Evolution and Lifetime of Intrinsic Magnetic Fields of Super-Earths in Habitable Zones. *ApJ* **726**, 70–87.
Tarduno, J. A., R. D. Cottrell, M. K. Watkeys, A. Hofmann, P. V. Doubrovine, E. E. Mamajek, D. Liu, D. G. Sibeck, L. P. Neukirch, and Y. Usui 2010. Geodynamo, Solar Wind, and Magnetopause 3.4 to 3.45 Billion Years Ago. *Science* **327**, 1238–1240.
Udry, S., X. Bonfils, X. Delfosse, T. Forveille, M. Mayor, C. Perrier, F. Bouchy, C. Lovis, F. Pepe, D. Queloz, and J.-L. Bertaux 2007. The HARPS search for southern extra-solar planets. XI. Super-Earths (5 and 8 $M_\oplus$) in a 3-planet system. *A&A* **469**, L43–L47.
U.R. Christensen, personal communication, U. R. 2011. Personal communication.
Valencia, D., M. Ikoma, T. Guillot, and N. Nettelmann 2010. Composition and fate of short-period super-Earths. The case of CoRoT-7b. *A&A* **516**, A20.
Valencia, D., and R. J. O'Connell 2009. Convection scaling and subduction on Earth and super-Earths. *Earth and Planetary Science Letters* **286**, 492–502.
Valencia, D., R. J. O'Connell, and D. Sasselov 2006. Internal structure of massive terrestrial planets. *Icarus* **181**, 545–554.
Valencia, D., R. J. O'Connell, and D. D. Sasselov 2007. Inevitability of Plate Tectonics on Super-Earths. *ApJL* **670**, L45–L48.
Valencia, D., D. D. Sasselov, and R. J. O'Connell 2007a. Detailed Models of Super-Earths: How Well Can We Infer Bulk Properties? *ApJ* **665**, 1413–1420.
Valencia, D., D. D. Sasselov, and R. J. O'Connell 2007b. Radius and Structure Models of the First Super-Earth Planet. *ApJ* **656**, 545–551.
van Hoolts, T. 2009. *Treatise on Geophysics*, Volume 10, Chapter The Rotation of the Terrestrial Planets, pp. 123–164. Elsevier.
van Thienen, P., K. Benzerara, D. Breuer, C. Gillmann, S. Labrosse, P. Lognonné, and T. Spohn 2007. Water, Life, and Planetary Geodynamical Evolution. *Space Sci. Rev.* **129**, 167–203.
Varga, P., C. Denis, and T. Varga 1998. Tidal friction and its consequences in palaeogeodesy, in the gravity field variations and in tectonics. *Journal of Geodesy* **25**, 61–84.
von Bloh, W., C. Bounama, M. Cuntz, and S. Franck 2007. The habitability of super-Earths in Gliese 581. *A&A* **476**, 1365–1371.

Symbol	Meaning	Notes
	Acronyms	
PMF	Planetary Magnetic Field	Surface magnetic field
CMF	Core Magnetic Field	Core surface magnetic field
CTE	Core Thermal Evolution	Gaidos *et al.* (2010)
MTE	Mantle based Thermal Evolution	Tachinami *et al.* (2011)
HZ	habitable zone	Kasting *et al.* (1993)
	Planetary Properties	
R_p	Planetary radius, $R_p = 6371(M/\,M_\oplus)^{0.265}$	km, Valencia *et al.* (2006)
R_c	Radius of the core, $R_c = 3480(M/\,M_\oplus)^{0.243}$	km, Valencia *et al.* (2006)
$\overline{\rho}_c$	Average core density, $\overline{\rho}_c = 1.1 \times 10^4 (M/\,M_\oplus)^{0.271}$	kg m^{-3}, Valencia *et al.* (2006)
Ω,T	Rotation rate, period of rotation, $T = 2\pi/\Omega$	rad s^{-1}, days
R_{ic}, χ	Radius of the solid inner core, $\chi = R_{ic}/R_c$	km
D	Vertical height of the liquid core, $D = R_c - R_{ic}$	km
V	Volume of the dynamo region, $V = 4/3\pi(R_c^3 - R_{ic}^3)$	km^3
	Dynamo Properties	
Q_{conv}	Total convective power	Ws^{-1}
p	Total convective power density	Adimensional
Lo	Lorentz number, $Lo \sim< E_{mag} >^{1/2}$	Adim., Christensen and Aubert (2006)
Ro	Rossby number, $Ro \sim< E_{kin} >^{1/2}$	Adim., Christensen and Aubert (2006)
Ro_l	Local Rossby number, $Ro_l \sim< l_u >< E_{kin} >^{1/2}$	Adim., Christensen and Aubert (2006)
f_{ohm}	Fraction of ohmic dissipation	Adim., Christensen and Aubert (2006)
	Magnetic Field Properties	
B_{rms}	rms amplitude of the magnetic field inside the convecting shell	μT
$\overline{B}_{dip}$	Dipolar component intensity of the CMF	μT
$\overline{B}_{s,dip}$	Dipolar component of the PMF, $\overline{B}_{s,dip} = \overline{B}_{dip}(R_c/R_p)^3$	μT
f_{dip}	Dipolar fraction of the CMF, $f_{dip} = \overline{B}_{dip}/\overline{B}_{CMB}$	Adim., Christensen and Aubert (2006)
b_{dip}	Ratio between the rms strength of the field and the dipolar component at the CMB, $b_{dip} = B_{rms}/\overline{B}_{dip}$	Adim., Christensen *et al.* (2009)
t_{ic}	Starting time for the inner core nucleation	Gyrs
T_{dip}	Dipolar lifetime	Gyrs
t_{sw}	Dipolarity switch time	Gyrs
T_{dyn}	Dynamo lifetime	Gyrs

Table 1: Symbols and quantities used in this work.

Appendix A. From the CMF to the PMF intensity

Assuming a low conductivity mantle and neglecting other field sources, the magnetic field in the region outside the conducting core is derived from a potential given by the solution of the Laplace equation with Neumann's boundary conditions at the CMB (Backus *et al.*, 1996),

$$V(r,\theta,\phi) = -\frac{R_c}{\mu_0}\sum_{l=1}^{\infty}\left(\frac{R_c}{r}\right)^{l+1}\sum_{m=0}^{l} a_l^m Y_l^m(\theta,\phi) \tag{A.1}$$

where Y_l^m are the spherical harmonics and a_l^m are the expansion coefficients. Using the harmonic expansion, the field regime (dipolar or multipolar) could be described in terms of the power spectrum $W_l(r)$ that expands the energy density at radius r,

$$W(r) = \sum_{l=1}^{\infty} W_l(r) \sim \sum_{l=1}^{\infty}\left(\frac{R_c}{r}\right)^{2l+4} w_l \tag{A.2}$$

CTE model (t_{ic},B_s,T_{dyn})

M ($M_\oplus$)	Tectonics	T_s 288K	T_s 1500K
$1\,M_\oplus$	PT	**2.8, 90, >10**	1.7,140,>10
	SL	6.5, 0, >10	5.9, 0, >10
$1.5\,M_\oplus$	PT	**4.4, 20, >10**	2.7, 130, >10
	SL	–	6.5, 0, >10
$2\,M_\oplus$	PT	**6.8, 20, >10**	4.2, 90, >10
$2.5\,M_\oplus$	PT	**>10, 20, 7**	>10, 30, 6.4
$3.0\,M_\oplus$	PT	**>10, 20, 6.5**	>10, 30, 10
$4.0\,M_\oplus$	PT	**>10, 20, 5.2**	>10, 30, 9

MTE model (t_{ic},B_s,T_{dyn})

M ($M_\oplus$)	V^*	ΔT_{CMB} 1000K	2000K	5000K	10000K
$1.0\,M_\oplus$	3 m^3 mol^{-1}	4, 80, >20	6.5, 110, >20	7.5, 130, >20	7.5, 130, >20
	10 m^3 mol^{-1}	**2.7, 80, 10**	2.8, 80, 10	2.8, 80, 10	2.8, 80, 10
$2.0\,M_\oplus$	3 m^3 mol^{-1}	0, 90, >20	7, 120, >20	8, 140, >20	**8, 140, >20**
	10 m^3 mol^{-1}	0, 0, 0.5	14, 100, >20	14, 100, >20	14, 100, >20
$5.0\,M_\oplus$	3 m^3 mol^{-1}	0, 0, 1	7.5, 130, >20	11, 160, >20	**11, 160, >20**
	10 m^3 mol^{-1}	0, 0, >20	>20, 0, >20	>20, 150, >20	>20, 150, >20

Table 2: Summary of results for the evolution of PMF in the CTE and MTE models (Gaidos *et al.*, 2010; Tachinami *et al.*, 2011). For every mass and each pair of independent planetary properties (tectonics and surface temperature, T_s in CTE model, activation volume, $V*$ and temperature contrast at CMB, ΔT_{CMB} in MTE model), we present the value of three properties of the dynamo and the predicted PMF: t_{ic} (Gyrs) the time for the starting of the inner core nucleation, $B_s(t_o)$ (μT) surface magnetic field at a reference time taken here as the present age of the Earth, 4.54 Gyrs and T_{dyn} (Gyrs) the lifetime of the dynamo. All the values are approximated and have been used to characterize the global conditions to have a protective PMF. In the CTE model stagnant lid (SL), as opposed to plate tectonics (PT) configurations, are not able to produce a dynamo for masses larger than 1.5 $M_\oplus$ and are not included in the Table. We have highlighted the configurations used in this work to study the role of rotation in the PMF evolution.

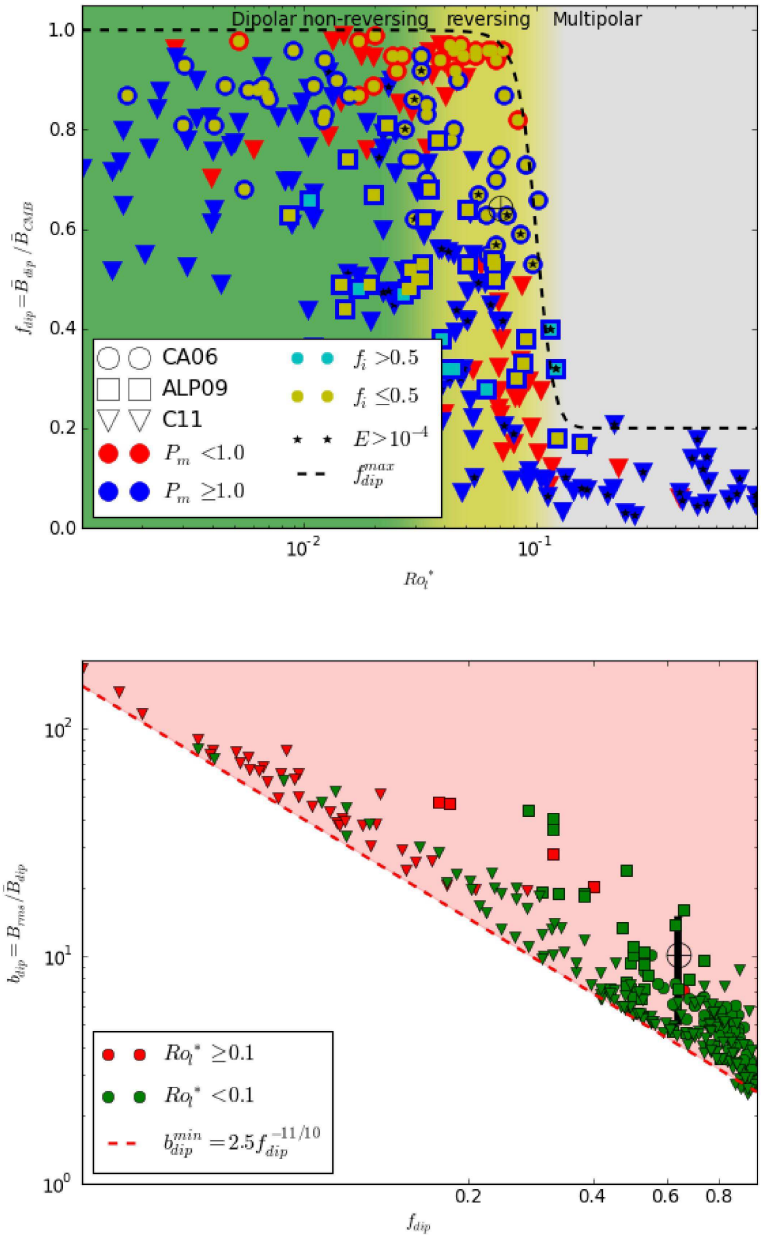

Figure 1: Upper panel: observed values of the f_{dip} ratio in numerical dynamo experiments. CA06, ALP09 and C11 stand for data obtained from Christensen and Aubert (2006), Aubert *et al.* (2009) and U.R. Christensen, personal communication (2011) respectively. The dashed curve is the maximum value of f_{dip} attainable at a given value of the local Rossby number. The regions corresponding to different dynamo regimes have been schematically depicted using shading vertical bands. Given the general complexity of the problem either multipolar dynamos could be found in the shaded region of reversing dipolar dynamos or non reversing dynamos ($f_{dip} \sim 1$) with certain boundary conditions could be found in the reversing band. Lower panel: values of b_{dip} and f_{dip} for the same set of numerical dynamo results used in the upper panel. A correlation between the minimum value of b_{dip} at a given value of f_{dip} is used in this work to estimate the maximum value of the dipolar component of the CMF (see text). The position of the geodynamo is indicated with the symbol $\oplus$. In the lower panel the uncertainty in $b_{dip\oplus}$ is indicated with the thick black line.

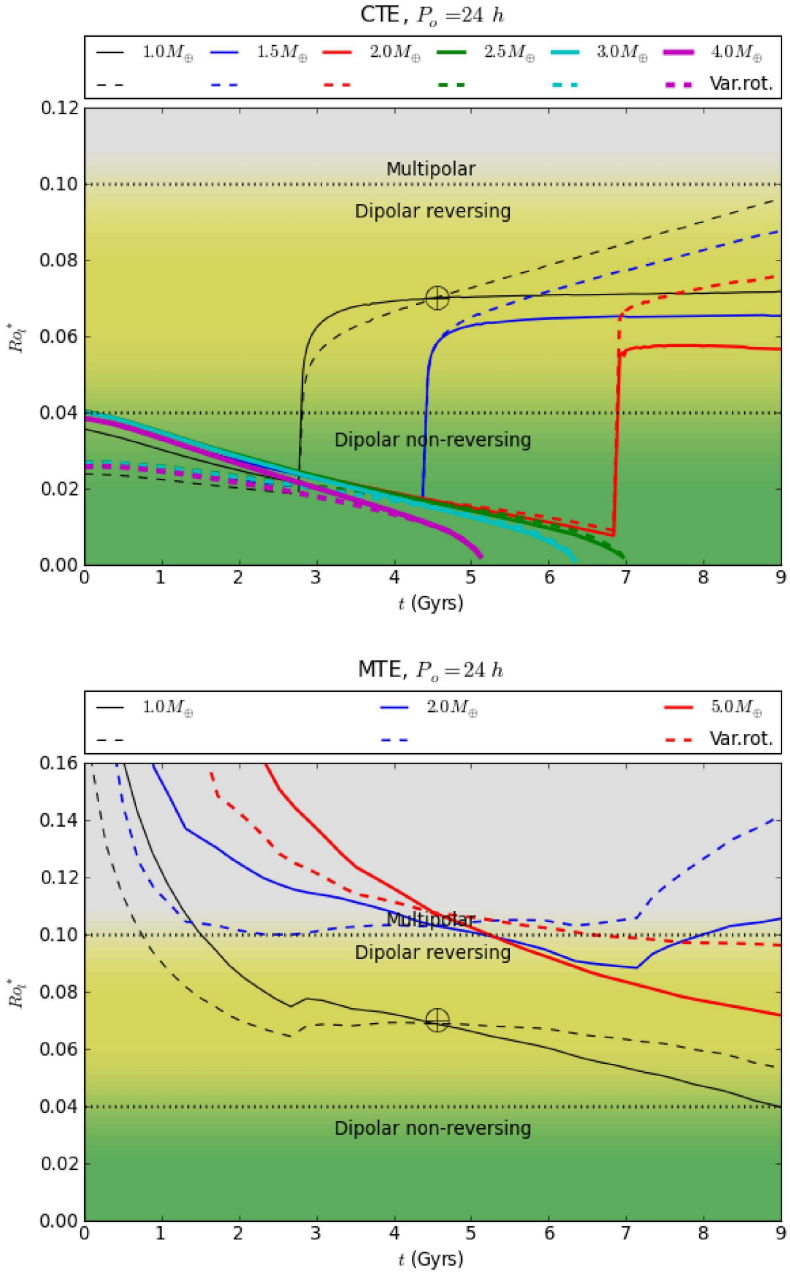

Figure 2: Evolution of the local Rossby number computed from selected results of the CTE (upper panel) and MTE (lower panel) models. Solid and dashed lines correspond to the cases of constant and variable period of rotation respectively. Earth-like values for the period of rotation were assumed, i.e. P_o=24 h and $t_o = 4.54$ Gyrs. In the case of a variable period of rotation (dashed lines) we have used $\dot{P}_o = 1.5$ h Gyrs^{-1}. Shaded regions enclose values of Ro_i^* corresponding to multipolar (gray upper region), dipolar reversing (yellow middle region) and dipolar non-reversing (green lower region) dynamo regimes.

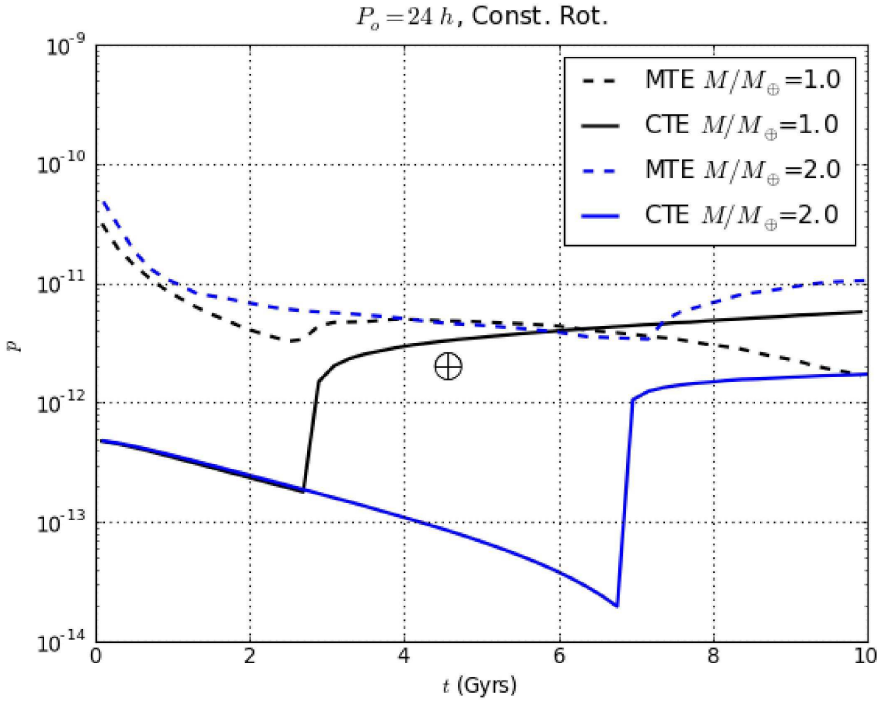

Figure 3: Evolution of the convective power density p in the CTE (solid lines) and MTE (dashed lines) models for two different planetary masses. p is one order of magnitude larger in the MTE model and falls faster than in the CTE model due to differences in the estimations of the convective power.

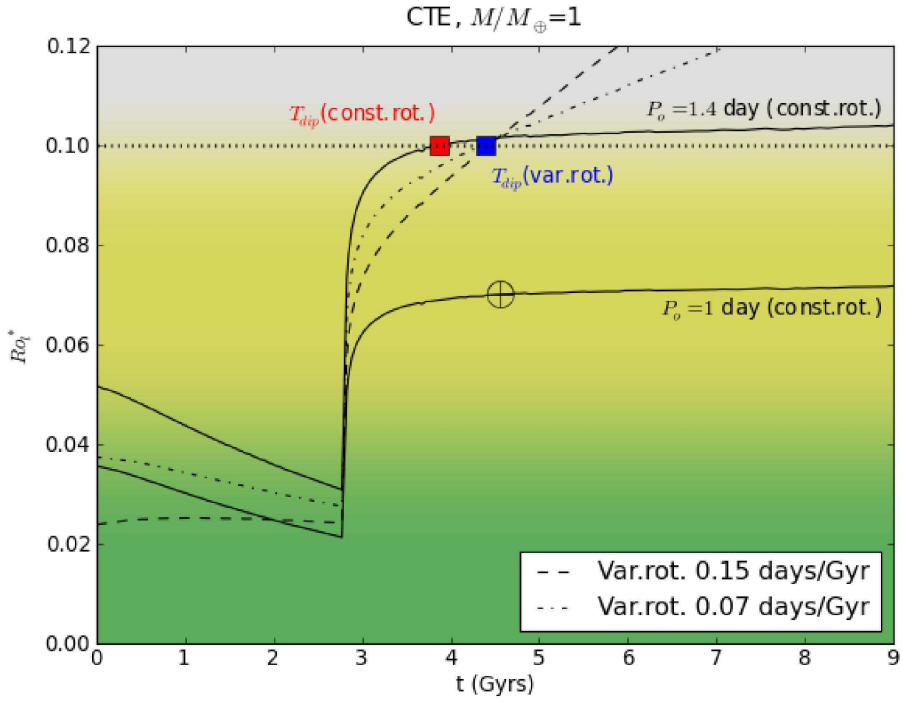

Figure 4: Comparison of the evolution of Ro_l^* for a $1\,M_\oplus$ planet with a period of rotation $P \approx 1.4$ days and $P \approx 1$ day in the CTE model. The Ro_l^* in the case of variable period of rotation (dashed and dashed-dotted lines) has been computed for two different rates $\dot{P}_o$ assuming the same reference period of rotation $P_o \approx 1.4$ days at $t = 4.54$ Gyrs. The squares are placed at the times where the dynamo becomes multipolar (dotted line at $Ro_l^* = 0.1$ marks the transition to the multipolar regime) for the constant and variable period of rotation cases respectively. Notice that the dashed line is below the dashed-dotted line before $t = 4.54$ Gyrs and above it after that time. Shaded regions enclose values of Rol* corresponding to different dynamo regimes, multipolar (upper region, $Ro_l^* > 0.1$), dipolar reversing (middle region, $0.04 < Ro_l^* < 0.1$) and dipolar non-reversing (lower region, $Ro_l^* < 0.04$).

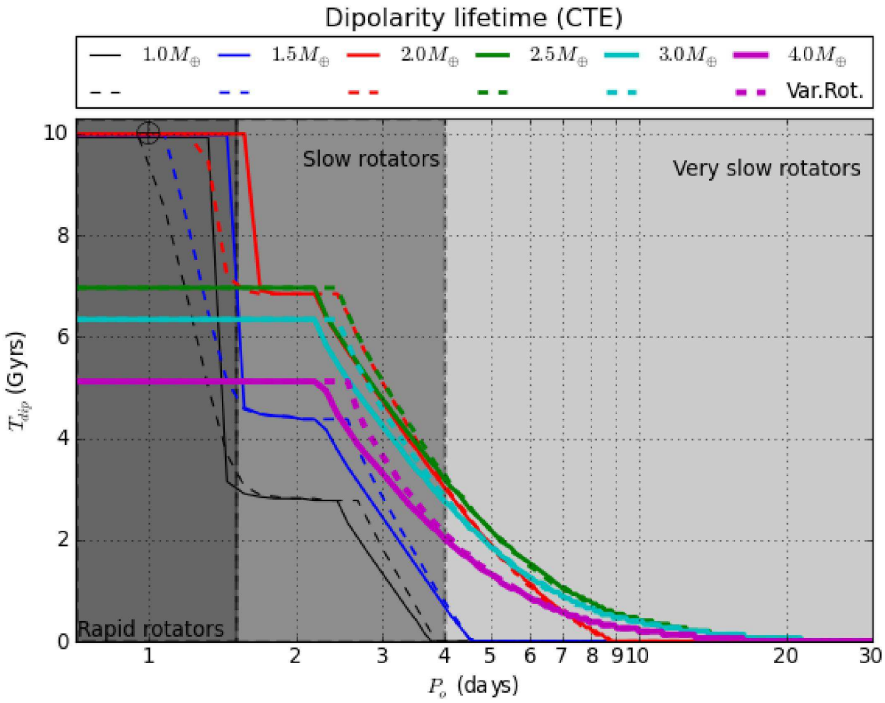

Figure 5: Lifetime of the dipolar dominated CMF in the CTE model obtained from the analysis of the Ro_l^* evolution for planets with different masses. Constant (solid line) and variable (dashed lines) periods of rotation have been assumed. The gray regions are limited by the maximum rotation periods of low mass planets ($M < 2\,M_\oplus$) in the three categories introduced in this work (see text).

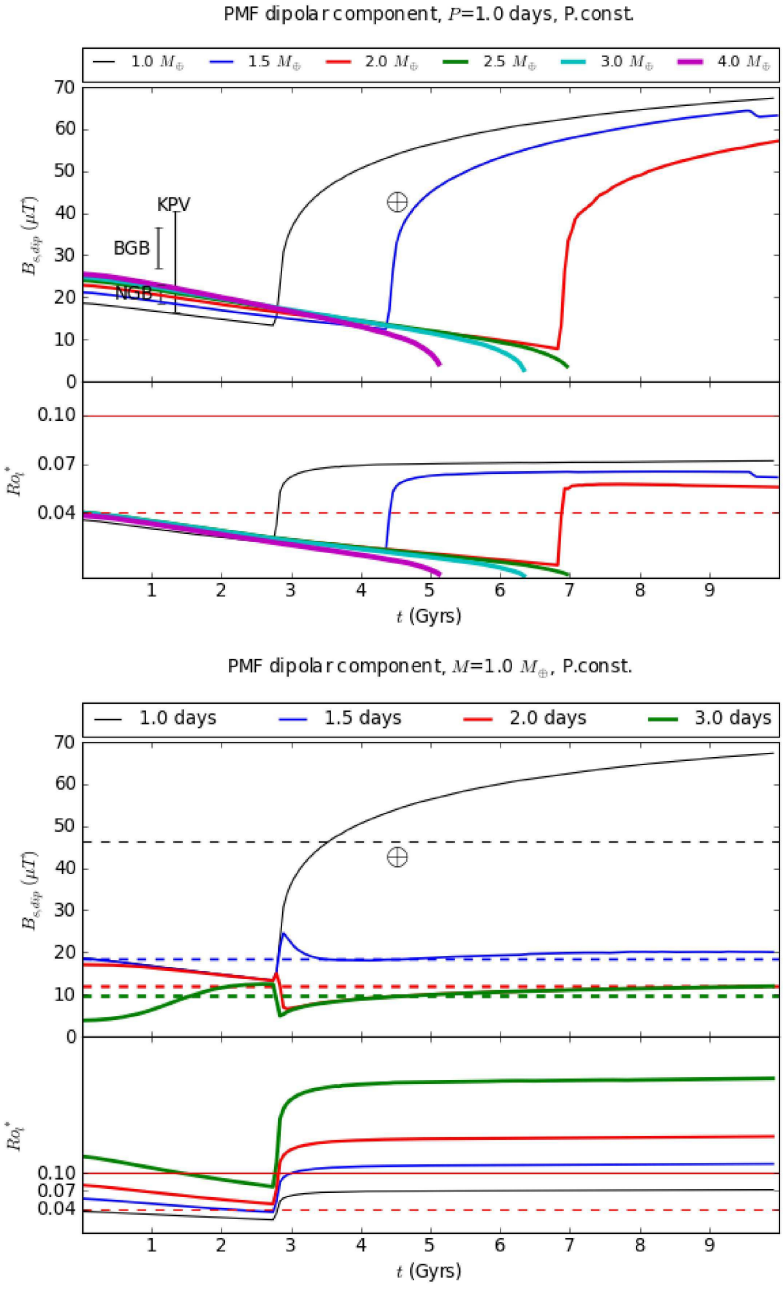

Figure 6: Maximum dipolar component of the surface PMF estimated with the procedure devised in this work and using the thermal inputs of the CTE model. In the upper panel the case of rapidly rotating planets, $P_o = 1$ day, is presented. In the lower panel the dipolar PMF intensities for a 1 $M_\oplus$ planet with different periods of rotation are compared. The value of the Ro_l^* has also been plotted in order to illustrate the effect that a transition between dynamo regimes have in the evolution of the PMF. The red continuous, dashed and dotted lines in the Ro_l^* subpanels are the limits between the regimes (dipolar non reversing, dipolar reversing and multipolar). In the lower panel, the dashed lines in the magnetic field plot are the lifetime average of the maximum dipolar component of the PMF, B_{avg} (Eq. (16)). The value of $B_{s,dip}$ for the present Earth's magnetic field (Earth symbol $\oplus$) and recent paleointensities measurements (error bars) has also been included (Tarduno *et al.* 2010: Kaap Valley (KVP), Barberton Greenstone Belt (BGB), and Nondweni Greenstone Belt (NGB), dacite localities).

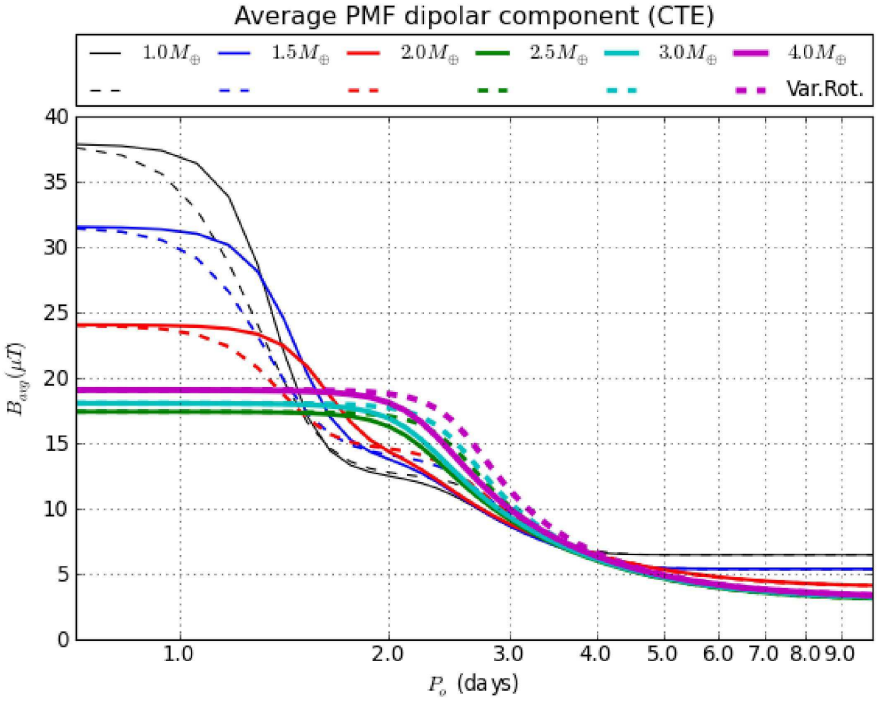

Figure 7: Surface dipolar field intensity averaged over the dynamo lifetime, B_{avg} as defined by Eq. (16), for planets with constant (solid) and variable (dashed lines) periods of rotation.

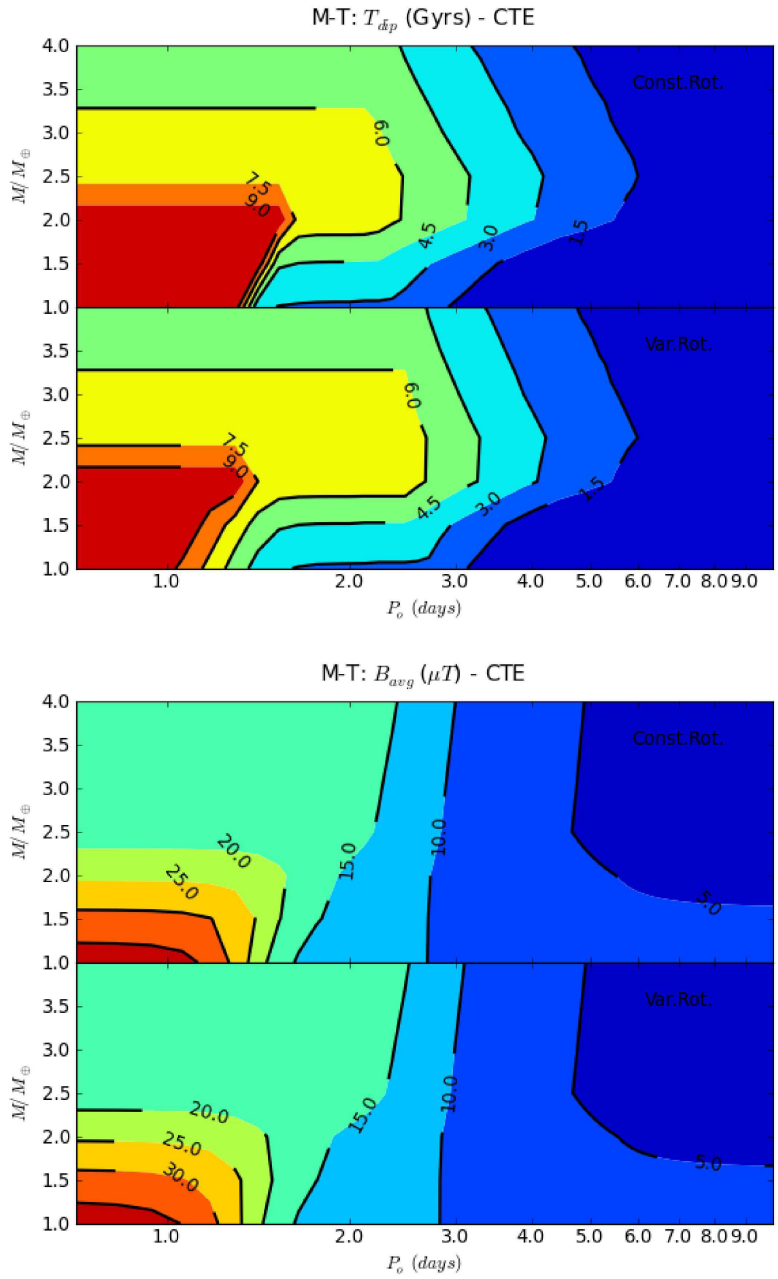

Figure 8: Mass-Rotation (M-P) diagrams for the dipolar field lifetime, T_{dip} and the average surface magnetic field, B_{avg} in the CTE model. In each diagram the case for constant (upper half of each panel) and variable (lower half of each panel) periods of rotation have been assumed. Contours of equal values of the quantities represented on each diagram are also included.

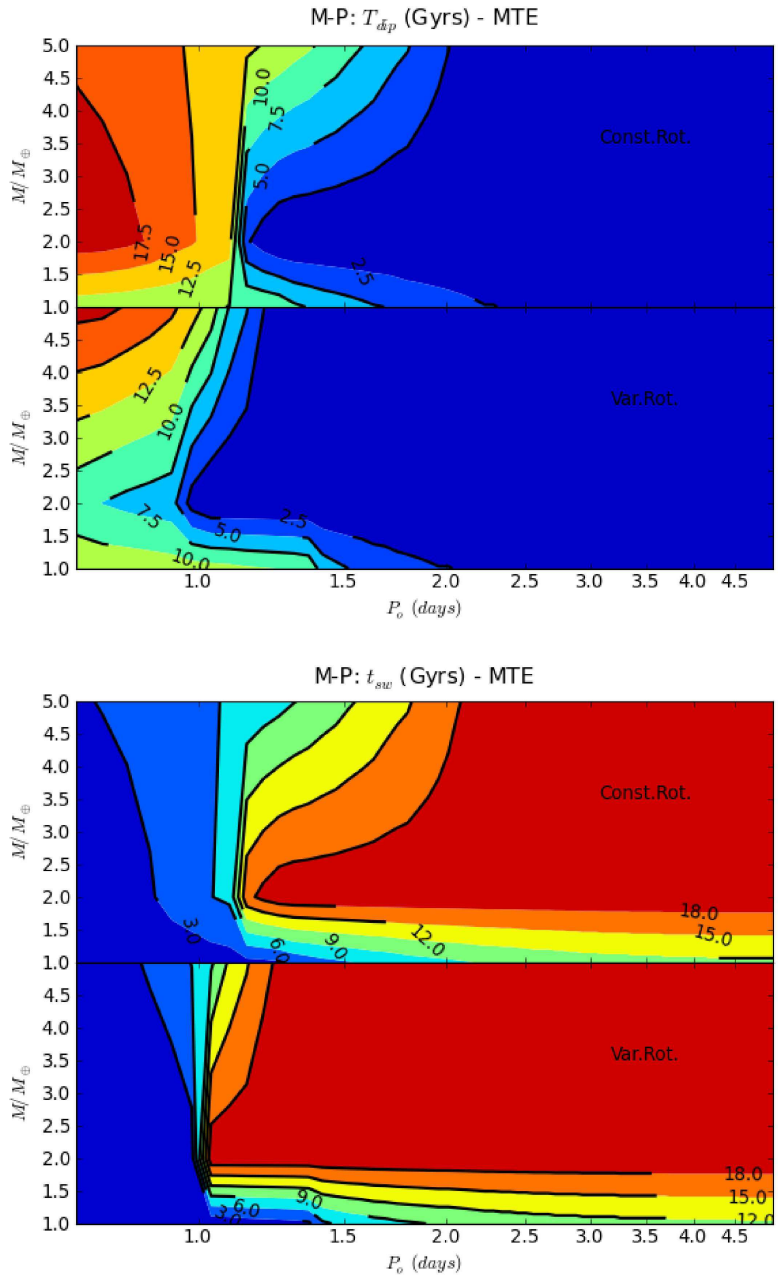

Figure 9: Mass-Rotation (M-P) diagrams for the dipolar field lifetime, T_{dip} and the dipolarity switch time t_{sw} in the MTE model. In each diagram the case for constant (upper half of each panel) and variable (lower half of each panel) periods of rotation have been assumed. Contours of equal values of the quantities represented on each diagram are also included.

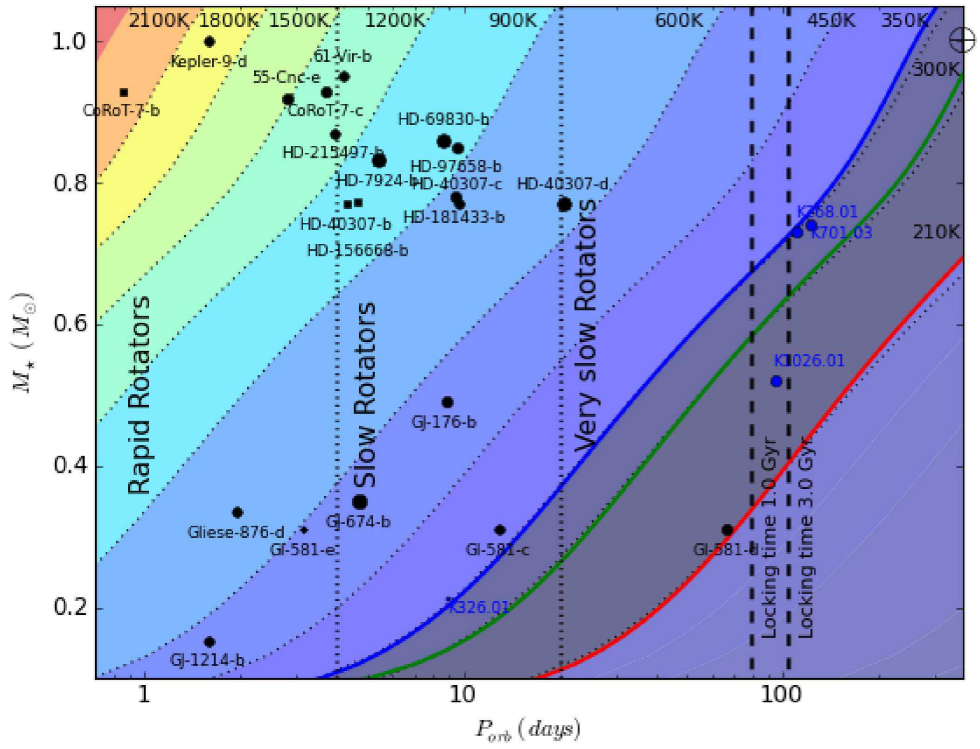

Figure 10: Stellar mass vs. orbital period diagram for planets around GKM stars ($M < 1.05 M_\odot$). Circles indicate the position of 21 of the known SEs and 4 Kepler candidates orbiting stars in the selected mass range. Each circle has a diameter proportional to the minimum mass of the planet. Contours of equal equilibrium temperatures T_{eq} as measured in planetary surfaces assuming an Earth-like bond albedo ($A = 0.29$) and a redistribution factor of 2 as expected for tidally locked planet (Selsis *et al.*, 2007) has been also plotted. Blue and red lines are the inner and outer limit of the habitable zone as computed using the Venus and Mars criteria in (Selsis *et al.*, 2007). Green line is the 1 AU-equivalent distance where the planet will receive the same flux as the Earth (Kaltenegger, 2010). The vertical thick dashed line indicates the maximum distance inside which planets will be tidally locked in times less than 1 and 3 Gyrs (Kasting *et al.*, 1993).

In the case of a dipolar dominated CMF, i.e. a magnetic field where the averaged dipolar component is a significative fraction of the total averaged magnetic field strength (see section 3.2), the dipolar contribution to the power spectrum $W_1(R_c) = w_1$ is generally larger than those from higher order harmonics (see for example the CMF power spectrum of the Earth and other simulated dynamos in Fig. 4 of Driscoll and Olson (2009)). Conversely when the field is multipolar the contribution from w_1 is of the same order or smaller than the higher order harmonics contributions. The dependence on r of $W_l(r)$ changes the power spectrum of the field outside the core. If the CMF is dipolar dominated, the surface field will be strongly dipolar. However, in the case of a multipolar field the surface field regime will depend on the CMB power spectrum. Multipolar fields with a flat spectrum $w_1 \simeq w_l$ for $l > 1$ will be dipolar on the planetary surface. A strongly multipolar field with a dominated component of order l_{max} will exhibit a surface flat spectrum provided $w_{lmax} \simeq w_1(R_c/R_p)^{2-2l_{max}}$. Assuming a quadrupole dominated CMF and $R_c/R_p \approx 0.3$ this conditions implies that for $w_2 \lesssim 10w_1$ the surface field will still be weakly dipolar.
The magnetic field outside of the core $\vec{B}(r,\theta,\phi) = -\nabla V(r,\theta,\phi)$ could also be expanded,

$$\vec{B}(r) = \sum_{l=1}^{\infty} \sum_{m=0}^{l} \vec{B}_l^m(r) \tag{A.3}$$

The contribution of order l is $\vec{B}_l(r) = \sum_{m=0}^{l} \vec{B}_l^m(r) = \vec{B}_l(R_c)(R_c/r)^{l+2}$. Using this notation the dipolar component of the CMF is written as $\overline{B}_{dip} =< |\vec{B}_1(R_c)| >$ where the average is computed over the CMB surface. On the planetary surface the dipolar component of the PMF will be then given by,

$$\overline{B}_{s,dip} = \overline{B}_{dip} \left(\frac{R_c}{R_p} \right)^3 \tag{A.4}$$

irrespective of the regime of the surface field.